

Dear Author,

Please, note that changes made to the HTML content will be added to the article before publication, but are not reflected in this PDF.

Note also that this file should not be used for submitting corrections.



ELSEVIER

Contents lists available at ScienceDirect

Annual Reviews in Control

journal homepage: www.elsevier.com/locate/arcontrol

Review

Overview of modelling and control strategies for wind turbines and wave energy devices: Comparisons and contrasts

J.V. Ringwood^a, S. Simani^{b,*}^a Centre for Ocean Energy Research, Maynooth University, County Kildare, Ireland^b Department of Engineering, University of Ferrara, Via Saragat 1E – 44123 Ferrara (FE), Italy

ARTICLE INFO

Article history:

Received 1 June 2015

Accepted 18 August 2015

Available online xxx

Keywords:

Wind turbines

Wave energy devices

Nonlinear modelling

Model-based control

Actuators and measurements

ABSTRACT

Increasingly, there is a focus on utilising renewable energy resources in a bid to fulfil increasing energy requirements and mitigate the climate change impacts of fossil fuels. While most renewable resources are free, the technology used to usefully convert such resources is not and there is an increasing focus on improving the conversion economy and efficiency. To this end, advanced control technology can have a significant impact and is already a relatively mature technology for wind turbines. Though wave energy systems are still in their infancy, significant benefits have been shown to accrue from the appropriate use of control technology. To date, the application communities connected with wind and wave energy have had little communication, resulting in little cross fertilisation of control ideas and experience, particularly from the more mature wind area to wave. This paper examines the application of control technology across both domains, both from a comparative and contrasting point of view, with the aim of identifying commonalities in control objectives and potential solutions. Key comparative reference points include the articulation of the stochastic resource models, specification of control objectives, development of realistic device models, and development of solution concepts. Not least, in terms of realistic system requirements are the set of physical and legislative constraints under which such renewable energy systems must operate, and the need to provide reliable and fault-tolerant control solutions, which respect the often remote and relatively inaccessible location of many offshore deployments.

© 2015 International Federation of Automatic Control . Published by Elsevier Ltd. All rights reserved.

1 Introduction

With the continuing decrease in the stock of global fossil fuels, issues of security of supply, and pressure to honour greenhouse gas emission limits (e.g., the Kyoto protocol), much attention has turned to renewable energy sources to fulfil future increasing energy needs. Wind energy, now a mature technology, has had considerable proliferation, with other sources, such as biomass, solar, and tidal, enjoying somewhat less deployment. Waves provide previously untapped energy potential and wave energy has been shown to have some favourable variability properties (a perennial issue with many renewable, especially wind), especially when combined with wind energy [Fusco, Nolan, and Ringwood \(2010\)](#).

While wind and wave energy share certain characteristics *i.e.* the raw resource is both free and somewhat unpredictable, their development has followed quite different paths, especially regarding

the level of maturity achieved. Wind farms, both offshore and on-shore, are now commonplace, and wind turbine design, with a few exceptions, has largely converged on the horizontal-axis device. In contrast, at the time of writing, no commercial wave farms are in existence, though a number of commercial wave farms are currently under development. In addition, the current poor state of wave-energy technology development is highlighted by the availability of just a few commercially available Wave-Energy Converters (WECs), including the Wave Dragon [Soerensen \(2003\)](#), Pelamis [Yemm, Pizer, and Retzler \(0000\)](#), Oyster [Whittaker and Folley \(2012\)](#), the SeaBased device [Leijon and Bernhoff \(2006\)](#) and Wavestar [Kramer, Marquis, and Frigaard \(2011\)](#). The stark contrast in the operational principles of these five devices, as well as the diversity in appearance and operation of the 147 prototypes listed in [Koca et al. \(2013\)](#), provides further evidence of the relative immaturity of wave-energy technology.

One common misconception, in effective renewable energy converter design, is that converters must be optimally efficient. However, since the resource itself (wind and wave) is free, the main objective is to minimise the converted cost of the renewable energy *i.e.* the cost per kWh, taking into account the lifetime costs (capital, operational and commissioning/decommissioning costs) as well as energy

* Corresponding author.

E-mail addresses: john.ringwood@eeng.nuim.ie (J.V. Ringwood),silvio.simani@unife.it (S. Simani).URL: <http://www.silviosimani.it> (S. Simani)

receipts (value of energy sold). Nevertheless, for a given capital cost, maximising the energy receipts (assuming relative insensitivity of operational costs) is an important economic objective and control system technology has an important role to play in this regard. In an ideal world, one should consider the design of a complete system from the top down. However, convention has it that physical systems are usually designed by the discipline-specific experts and the control problem is then addressed in a subsequent step by control engineers, working in collaboration with the discipline-specific experts. Such an approach, though prevalent in the bulk of industrial applications of control, is non-optimal, even if there are some notable exceptions. Some preliminary studies do suggest a strong interaction between the fundamental design of renewable energy conversion machines and the algorithms and systems used to control them, both for the wind [Bianchi, Battista, and Mantz \(2007\)](#), [Pao and Johnson \(2011\)](#) and wave [Garcia-Rosa, Bacelli, and Ringwood \(2015a\)](#), [Garcia-Rosa and Ringwood](#) cases. In any case, given the relatively low cost of control systems technology (sensors, actuators, computer, software) compared to the cost of the renewable energy converters (approx. \$5m–\$16m/MW for wave, \$1.3m–\$2.2m/MW for wind [World Energy Council \(2013\)](#)), it will be assumed in this paper that the focus is on increasing the energy conversion capacity of a given wind or wave energy device. However, this relatively simple implementation modality masks both the capability of control systems and the high level of engineering underpinning the development of a suitable control algorithm. For example, many high-performance model-based control design methods require an accurate mathematical model of the system to be controlled and a significant number of man-hours can be absorbed in modelling. Nevertheless, there is usually a good case to be made for the incorporation of control technology to improve the performance (both technical and economic), reliability and safety of a system [Odgaard \(2012\)](#). By taking into account commonalities and contrasts in particular for wind turbines and wave energy devices, this work will consider the role that modelling and control engineering can play in making energy conversion systems more competitive and effective.

There are a number of economic issues associated with the introduction of control systems for renewable energy devices which need to be considered. One important factor is that many wind and wave devices are situated in relatively remote and/or inaccessible areas, with consequent implications for maintenance. As a result, the implemented control systems should be reliable and there is a need for fault-tolerant control [Blanke, Kinnaert, Lunze, and Staroswiecki \(2006\)](#), [Odgaard \(2012\)](#). In addition, any increases in duty cycle, velocities or forces associated with energy converter components need to be considered and these may impact operational cost via additional maintenance requirements.

Both wind turbines and wave energy devices exhibit nonlinear behaviour and are required to operate over a wide range of excitations. Wind and wave energy systems also have particular physical constraints (displacements, velocities, accelerations and forces) which must be strictly observed if such systems are to operate effectively and have economically attractive useful operational lifetimes. The motivation for this paper comes from a real need to have an overview on the modelling and control challenges for wind turbines and wave energy devices, which present common and different requirements related to renewable source power conversion efficiency into electric energy.

In general, in the fields considered in this paper, power conversion is converting renewable sources to electric energy, regulating also the voltage and frequency. Therefore, a power converter is an electro-mechanical device for converting wind/wave energy to electrical energy. The power converter includes an electrical machinery that is used to convert and control both frequency and voltage.

It is worth noting that the combination of wave and wind energy systems will not be considered in this paper, as addressed e.g.

in [Nolan and Ringwood \(2005\)](#), [Fusco et al. \(2010\)](#), [Teillant, Costello, Weber, and Ringwood \(2012\)](#). Moreover, floating wind turbine concepts, which present important and challenging aspects for both the modelling and control points of view, see e.g. [Matha \(2009\)](#), [Schlipf et al. \(2013\)](#), are also beyond the scope of the current review.

With this view, the work will focus on commonalities and contrasts for wind and wave energy systems. Wind turbine systems seem relatively mature from the modelling point of view, whilst wave energy devices present unique, interesting and challenging aspects. Therefore, the final aim is to see what modelling and control aspects might be common with a view to utilising some ideas, born in one domain, within the other. These issues have begun to stimulate research and development in the wider control community in each domain, and the main results will be summarised in this work. In particular, a proper mathematical description of these energy conversion systems should be able to capture the complete behaviour of the process under monitoring, thus providing an important impact on the control design itself.

Therefore, the analysis of the commonalities and the contrasts between these two fields will be performed according the following items, which describe also the structure of the paper:

- Requirements of the generic control problem: unique aspects to wind turbine and wave energy systems;
- Purpose of the models for wind turbines and wave energy systems;
- Models for the renewable resources: comparisons and contrasts of wave and wind model characteristics;
- Control strategy development: objectives and available tools for wind turbine and wave energy systems;
- Conclusions: are these two domains really comparable? On what basis – modelling and/or control, and/or the intermittent resource that drive them? Are there some fundamental issues, from a control perspective, that explain why wind turbines are now commonplace, but wave energy devices are not?

1.1. Overview of wind turbine systems

The main components of a horizontal-axis wind turbine that are visible from the ground are its tower, nacelle, and rotor, as can be seen in [Fig. 1](#). The nacelle houses the generator, which is driven by the high-speed shaft. The high-speed shaft is in turn usually driven by a gear box, which steps up the rotational speed from the low-speed shaft. The low-speed shaft is connected to the rotor, which includes the airfoil-shaped blades. These blades capture the kinetic energy in the wind and transform it into the rotational kinetic energy of the wind turbine [Bianchi et al. \(2007\)](#).

Wind turbine control goals and strategies are affected by turbine configuration [Munteanu and Bratcu \(2008\)](#). horizontal-axis wind turbines may be ‘upwind’, with the rotor on the upwind side of the tower, or ‘downwind’. The choice of upwind versus downwind configuration affects the choice of yaw controller and the turbine dynamics, and thus the structural design. Wind turbines may also be variable pitch or fixed pitch, meaning that the blades may or may not be able to rotate along their longitudinal axes. Although fixed-pitch machines are less expensive initially, the reduced ability to control loads and change the aerodynamic torque means that they are becoming less common within the realm of large wind turbines. Variable-pitch turbines may allow all or part of their blades to rotate along the pitch axis [Bianchi et al. \(2007\)](#), [Burton, Sharpe, Jenkins, and Bossanyi \(2011\)](#).

Moreover, wind turbines can be variable speed or fixed speed. Variable-speed turbines tend to operate closer to their maximum aerodynamic efficiency for a higher percentage of the time, but require electrical power processing so that the generated electricity can be fed into the electrical grid at the proper frequency. As

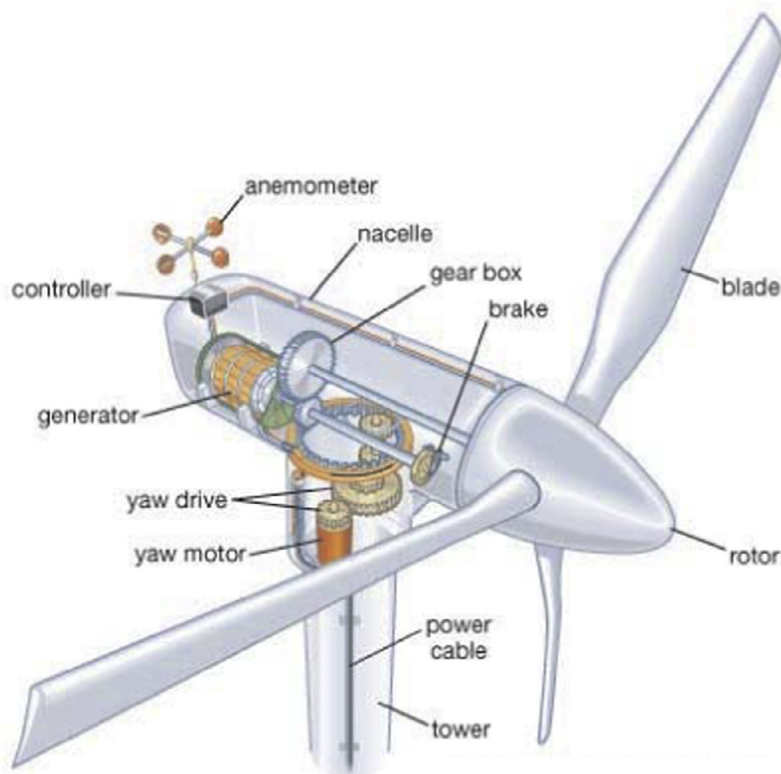


Fig. 1. Wind turbine main components.

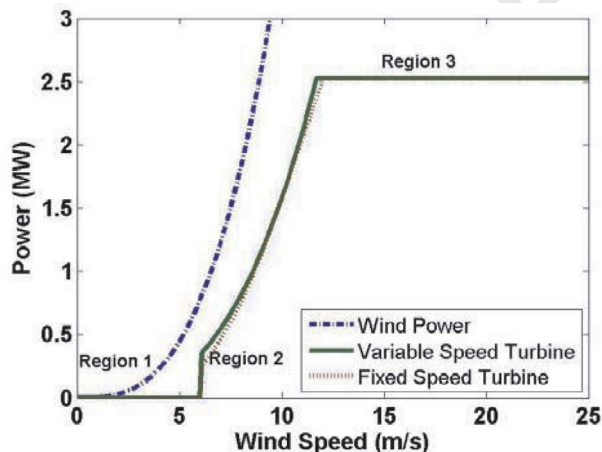


Fig. 2. Example power curves. The wind power curve shows the power available in the wind for a turbine of the same size as the two example turbines.

generator and power electronics technologies improve and costs decrease, variable-speed turbines are becoming more popular than constant-speed turbines at the utility scale Bianchi et al. (2007).

Fig. 2 shows example power curves for a variable-speed and a fixed-speed wind turbine, as well as a curve showing the power available in the wind for this 2.5 MWh example turbine. For both turbines, when the wind speed is low (in this case, below 6 m/s), the power available in the wind is low compared to losses in the turbine system so the turbines are not run. This operational region is sometimes known as Region 1. When the wind speed is high, Region 3 (above 11.7 m/s in this example), power is limited for both turbines to avoid exceeding safe electrical and mechanical load limits Odgaard, Stoustrup, and Kinnaert (2013).

Note that the example turbines in Fig. 2 produce no power in low winds because they are not turned on until the wind speed reaches a certain level. Further, power is limited to protect the electrical and mechanical components of both turbines in high wind speeds. Both turbines produce the same power at the design point for the fixed speed turbine, but the variable speed turbine produces more power over the rest of Region 2 Pao and Johnson (2009).

The main difference in Fig. 2 between the two types of turbines appears for mid-range wind speeds, Region 2, which encompasses wind speeds between 6 and 11.7 m/s in this example. Except for one design operating point (10 m/s in this example), the variable-speed turbine captures more power than the fixed-speed turbine. The reason for the discrepancy is that variable-speed turbines can operate at maximum aerodynamic efficiency over a wider range of wind speeds than fixed-speed turbines. The maximum difference between the two curves in Region 2 is 150 kWh. As shown in Section 2.1, for a typical wind speed distribution with a Weibull distribution, the variable-speed turbine captures 2.3% more energy per year than the constant-speed turbine, which is considered to be a significant difference in the wind industry.

Not shown in Fig. 2 is the 'high wind cut-out', a wind speed above which the turbine is powered down and stopped to avoid excessive operating loads. High wind cut-out typically occurs at wind speeds above 20–30 m/s for large turbines, with many factors determining the exact value.

Even a perfect wind turbine cannot fully capture the power available in the wind. In fact, actuator disk theory Froude (1889) (i.e. a theory used in fluid dynamics used for describing a mathematical model of an ideal actuator disk, such as an helicopter rotor) shows that the theoretical maximum aerodynamic efficiency, which is called the Betz Limit, is approximately 59% of the wind power Betz and Randall (1966). The reason that an efficiency of 100% cannot be achieved is that the wind must have some kinetic energy remaining

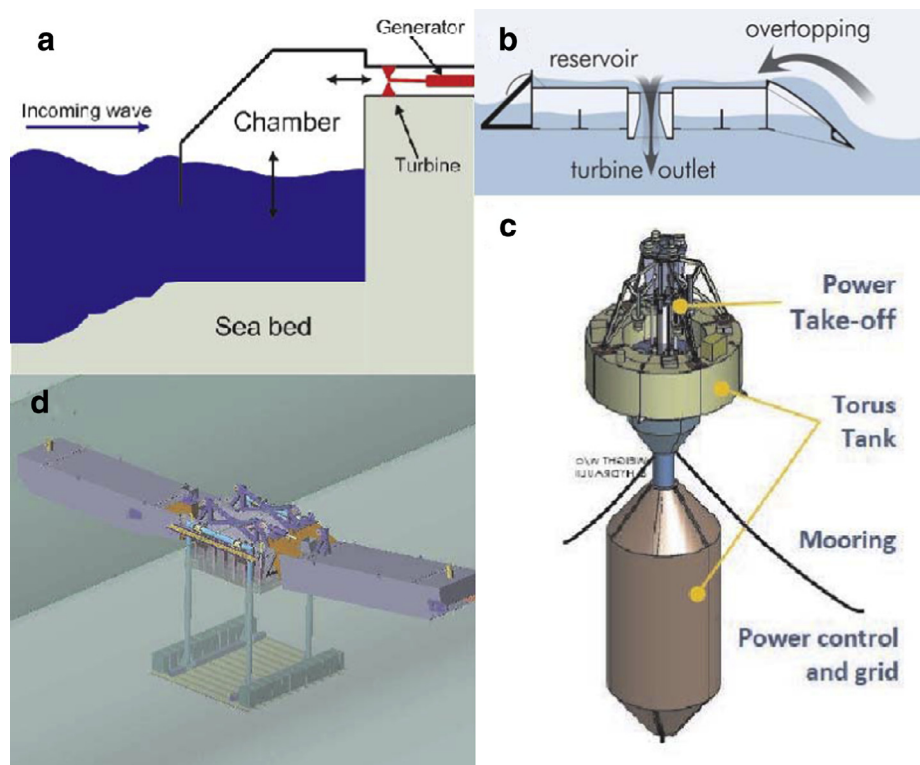


Fig. 3. Various WEC devices, based on diverse operating principles (a) OWC, (b) overtopping device, (c) self-reacting point absorber, (d) hinged-barge connected structure.

212 after passing through the rotor disc; if it did not, the wind would
 213 by definition be stopped and no more wind would be able to pass
 214 through the rotor to provide energy to the turbine.

215 The most common mathematical description of the complete
 216 wind turbine model will be provided in Section 3.2.

217 1.2. Overview of wave energy systems

218 Current wave energy prototype devices are diverse in operation
 219 and principle Koca et al. (2013), Drew, Plummer, and Sahinaya (2009).
 220 Some oscillating devices are shore-mounted and harness the motion
 221 of an enclosed Oscillating Water Column (OWC), while others oper-
 222 ate offshore and can be bottom or fixed platform referenced, or self-
 223 reacting multi-body structures. Others utilise overtopping of a float-
 224 ing reservoir to rectify the oscillating power flux of the waves. Fig. 3
 225 shows a small selection of WEC devices.

226 While operating principles vary, WECs usually rely on the hydro-
 227 dynamic wave force to create a variation in the displacement between
 228 the WEC and a (fixed or relatively fixed) reference. In some case, the
 229 reference is provided by the seabed while, in other cases, the varia-
 230 tion is between two components of the same device, tuned to reso-
 231 nate at different frequencies. In the OWC case, the water column
 232 itself provides the movement, with the body of the device remain-
 233 ing relatively fixed. The relative motion is then harnessed into a use-
 234 ful form using some form of pneumatic, hydraulic or electrical Power
 235 Take-Off (PTO) system.

236 Like wind turbines, wave energy devices have to operate under a
 237 wide variety of resource characteristics but, in the wave case, devices
 238 are subject to both wave amplitude and wave period variations. In ad-
 239 dition, there may be more extreme sea states where the device must
 240 be put into a ‘safe’ mode, where power production is abandoned and
 241 the device configured to minimise the likelihood of damage. There
 242 is also a need to ensure that the rated power of the electrical sys-
 243 tem is not exceeded in power production mode, articulated by the
 244 flat portion of a typical wind turbine power curve, as described in

245 Section 1.1. Since the wave period changes frequently, it is difficult
 246 to design a device to ‘resonate’ over all wave periods well; either a
 247 device in its natural form can resonate very well at a particular fre-
 248 quency, or it can resonate poorly across a wide band of frequencies.
 249 However, control systems may be employed to artificially adjust the
 250 resonant frequency of the device, preserving good power capture per-
 251 formance over a range of typical sea conditions. Unlike wind turbines,
 252 the power flux incident on a wave energy device is reciprocating,
 253 usually described (using linear wave theory) as a sum of sinusoids.
 254 However, like the wind turbine problem, there is a need to match the
 255 device load to the available excitation and this presents itself as an
 256 impedance-matching problem Ringwood, Bacelli, and Fusco (2014),
 257 compared to the resistance matching problem for wind turbines, re-
 258 flecting the unidirectional motion of wind turbines and the (usually)
 259 reciprocating motion of wave energy devices. Further clarification on
 260 the impedance matching problem is given in Section 4.3.1. This load
 261 matching is the effective means by which the resonant period of a
 262 WEC is altered. We can note that there is a significant interaction be-
 263 tween the control problem and the optimal geometric design (in par-
 264 ticular size) of the device, for a specific wave climate Garcia-Rosa and
 265 Ringwood.

266 In addition to adjusting the loading on the device, a WEC control
 267 system must also observe the physical constraints on a device, pri-
 268 marily force and excursion constraints. However, velocity and accel-
 269 eration constraints may also be relevant. In many cases, some control
 270 considerations can be used to optimise the trade-off between
 271 force and excursion constraints (noting that increased resisting force
 272 results in lower amplitude excursions) to maximise power capture
 273 Bacelli and Ringwood (2013c).

274 Like wind turbines, wave energy devices are deployed in farms, to
 275 maximise the economy of scale in the high costs associated with elec-
 276 trical infrastructure and mooring systems. Like wind farms, the objec-
 277 tive is to maximise the performance of the whole farm, considering
 278 the prevalent direction of the incoming wave resource. However, un-
 279 like wind farms, WECs operating in a farm structure produce both

		Power period (T_{pow} , s)																	
		5.0	5.5	6.0	6.5	7.0	7.5	8.0	8.5	9.0	9.5	10.0	10.5	11.0	11.5	12.0	12.5	13.0	
Significant wave height (H_{sig} , m)	0.5	idle	idle	idle	idle	idle	idle	idle	idle	idle	idle	idle	idle	idle	idle	idle	idle	idle	
	1.0	idle	22	29	34	37	38	38	37	35	32	29	26	23	21	idle	idle	idle	
	1.5	32	50	65	76	83	86	86	83	78	72	65	59	53	47	42	37	33	
	2.0	57	88	115	136	148	153	152	147	138	127	116	104	93	83	74	66	59	
	2.5	89	138	180	212	231	238	238	230	216	199	181	163	146	130	116	103	92	
	3.0	129	198	260	305	332	340	332	315	292	266	240	219	210	188	167	149	132	
	3.5	-	270	354	415	438	440	424	404	377	362	326	292	260	230	215	202	180	
	4.0	-	-	462	502	540	546	530	499	475	429	384	366	339	301	267	237	213	
	4.5	-	-	544	635	642	648	628	590	562	528	473	432	382	356	338	300	266	
	5.0	-	-	-	739	726	731	707	687	670	607	557	521	472	417	369	348	328	
	5.5	-	-	-	750	750	750	750	750	737	667	658	586	530	496	446	395	355	
	6.0	-	-	-	-	750	750	750	750	750	750	711	633	619	558	512	470	415	
	6.5	-	-	-	-	750	750	750	750	750	750	750	743	658	621	579	512	481	
	7.0	-	-	-	-	-	750	750	750	750	750	750	750	750	750	676	613	584	525
	7.5	-	-	-	-	-	-	750	750	750	750	750	750	750	750	750	686	622	593
	8.0	-	-	-	-	-	-	-	750	750	750	750	750	750	750	750	750	690	625

Fig. 4. Power matrix for the Pelamis wave power device.

destructive and constructive interference, since devices in motion radiate waves which can constructively interfere with the incident waves experienced by other devices. In fact, the farm containing n_d devices can have a better performance than n_d isolated devices, for particular wave directions and climates. As a result, the problem of controlling a WEC array does not reduce to the individual control of each device in the array, but should also consider the interactions between the devices, if maximum power capture is to be attained Bacelli, Balitsky, and Ringwood (2013a), Bacelli and Ringwood (2013a). In addition, a significant interaction between the optimal array layout and the control system has also been identified Garcia-Rosa et al. (2015a).

Since the power production of WECs is sensitive to both wave amplitude and period, power production characteristics are defined by two input parameters, sometimes articulated in the form of a look-up table, as shown in Fig. 4.

1.3. Specification of the generic control problem

In general, control science attempts to devise algorithms that force a system to follow a desired path, objective, or behaviour modality. Traditionally, the control problem is defined by a tracking problem, where the objective is for the system output to follow the reference input Kuo (1995). While problems of this type do occur in energy conversion applications, for example speed control of both wind and tidal turbines, it is useful to broaden the set of problem descriptions and potential solutions a little, in order to assess the potential of control engineering in the general energy conversion context.

In general, the control problem definition requires the maximisation or the minimisation of a prescribed performance objective (such as the max. energy, min. error) subject to proper system constraints (see e.g. amplitudes, rates, forces, etc) i.e. a constrained optimisation problem. The definition considered here is not inconsistent with the purpose of a classic controlled system with a feedback loop, where the objective function is usually some measure (e.g. a quadratic mea-

sure) of the difference between the controlled output and its desired value, i.e. the tracking error, with respect to the reference or the set-point. In this way, the desired performance of the tracking system in closed-loop can be specified in a variety of ways Kuo (1995):

1. Desired transient response;
2. Desired steady-state response;
3. Desired closed-loop poles (roots of the closed-loop transfer function);
4. Trade-off between control energy and tracking error;
5. Minimisation of the sensitivity of the closed-loop system to variations in the system description;
6. Minimisation of the sensitivity of the closed-loop system to external disturbances.

Items 5 and 6 in the list above relate to the system robustness and specific control methodologies to address these objectives have been developed since the late 1970s. In most cases, control design methods provide an explicit solution for the feedback controllers, while some methods solve the more general optimisation problem defined at each time step. In the following, specific or general solutions, which can be useful in the control of wind turbines and ocean energy devices, will be recalled and analysed.

We propose a generic control problem framework, as shown in Fig. 5, consisting of an upper (optimal) setpoint generation stage and a lower control loop to ensure tracking of the setpoint. Both sets of control calculations must be mindful of physical constraints in the system. In the wind energy case, for variable speed turbines, an optimal rotational speed is first calculated (for Regions 2–3 of the power curve in Fig. 2), and torque and/or blade pitch control used to achieve the required rotational speed. In the wave energy case, an optimal velocity profile is calculated for a device and the PTO system modulated to follow the desired velocity profile.

Note, finally, that many control methods require a mathematical model of the system, in order to determine the control algorithm and

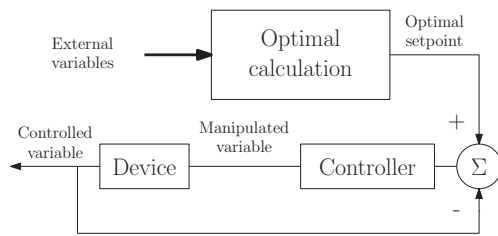


Fig. 5. Hierarchical control structure, showing the optimal setpoint (feedforward) calculation and the servomechanism section.

such methods are termed model-based. The requirement for an accurate mathematical system model often involves considerably more work than the calculation of the controller itself, though system identification techniques Simani, Fantuzzi, and Patton (2003), Fusco and Ringwood can be employed to determine a black-box model, *i.e.* a model which has no structural relationship to the physical system. The combination of system identification techniques with a mathematical procedure for controller determination can be used to develop adaptive controllers, which have the capability to adapt to unknown (in 'self-tuning mode') or time-varying systems. Adaptive control schemes based on linear system models also have the capability to track variations in a linear model due to the presence of nonlinearity, though nonlinear systems are best controlled with a dedicated fixed-parameter nonlinear controller. Significant care and attention must also be paid to adaptive schemes to ensure stability and convergence over all operating regimes Ioannou and Sun (1996).

1.3.1. Unique aspects to wind turbine systems

The goal in this tutorial is to introduce control engineers to the technical challenges that exist in the energy conversion industry and to encourage new modelling strategies and control systems research in this area. In fact, wind turbines are complex structures operating in uncertain environments and lend themselves nicely to advanced control solutions. Advanced controllers can help achieve the overall goal of decreasing the cost of wind energy by increasing the efficiency, and thus the energy capture, or by reducing structural loading and increasing the lifetimes of the components and turbine structures Bossanyi (2003).

Although wind turbines come in both vertical- and horizontal-axis configurations, the work will focus on Horizontal-Axis Wind Turbines (HAWTs). HAWTs have an advantage over Vertical-Axis Wind Turbines (VAWTs) in that the entire rotor can be placed atop a tall tower, where it can take advantage of larger wind speeds higher above the ground. Some of the other advantages of HAWTs over VAWTs for utility-scale turbines include pitchable blades, improved power capture and structural performance. VAWTs are much more common as smaller turbines, where these disadvantages become less important and the benefits of reduced noise and omni-directionality become more pronounced. Active control is most cost-effective on larger wind turbines, and therefore this work will refer to wind turbines with relatively large capacities. As remarked in Pao and Johnson (2009), active control refers to those active actions allowing conversion energy systems to achieve optimal power capture and structural performance, such as the use of pitchable blades, power and torque control techniques. On the other hand, the term active has been extended to fault diagnosis and fault tolerant control fields Chen and Patton (1999), Mahmoud, Jiang, and Zhang (2003), Zhang and Jiang (2008), Ding (2008), as outlined also in Section 5.1.

It is worth also noting that the mathematical description used for wind turbine modelling and control is quite basic, as the paper focusses on the related fundamental aspects. On the other hand, real system cases require much more complex modelling and control considerations, which have been highlighted through proper bibliographical references.

1.3.2. Unique aspects to wave energy systems

For ocean energy systems, the modelling effort can be considerable, since hydrodynamic modelling is involved. While a variety of comprehensive nonlinear modelling methodologies are available for hydrodynamic modelling, including Smooth Particle Hydrodynamics (SPH) or Computational Fluid Dynamics (CFD) approaches, the difficulty of incorporating such models into a control formulation suggests the use of more compact and structurally simple models. In addition, the very significant computational complexity of SPH or CFD models preclude their direct use for real-time controller implementation. Instead, model-based control strategies usually use compact linear models, which are based on either local linearisation about an operating point (see, for example, Bianchi et al., 2007; Leithead and Connor, 2000 for the turbine case, or linear boundary/element models Eriksson, Waters, Svensson, Isberg, and Leijon, 2007 for the wave energy case). Even modest nonlinear extensions to linear boundary element methods can result in models which are computationally intractable for real-time control Merigaud, Gillotheaux, and Ringwood (2012), while some specific parameterisations (*e.g.* to include viscosity effects Bhinder, Babarit, Gentaz, and Ferrant, 2012) give nonlinear parametric forms that may be possible to incorporate in model-based control schemes.

To summarise, WEC control systems must vary the PTO force in order to match the WEC to an incoming wave excitation in order to maximise power capture, mindful of physical constraints. If operating in an array, the WEC control system must also consider inter-device hydrodynamic coupling. In essence, the calculation of the optimal PTO force (or, more commonly, the optimal velocity profile for the WEC to follow) is a feed-forward problem, involving a calculation based on the some parameters of the incoming wave variations and the system model. Following this feedforward calculation, a traditional feedback controller is employed to ensure that the optimal velocity profile is followed.

2. Models for the renewable resources

In the following, the mathematical descriptions for the renewable resources that drive the models provided above will be briefly highlighted.

2.1. Wind models

The differential heating of the Earth's atmosphere is the driving mechanism for wind. Various atmospheric phenomena, such as the nocturnal low-level jet, sea breezes, frontal passages, and mountain and valley flows, affect the wind inflow across a wind turbine rotor plane Manwell, McGowan, and Rogers (2002), which spans from 60 to 180 m above the ground for megawatt utility-scale wind turbines. Given the large rotor plane and the variability of the wind, hundreds of sensors would be required to characterise the spatial variation of the wind speed encountered over the entire span of each blade.

The available wind resource can be characterised by the spatial or temporal average of the wind speed; the frequency distribution of wind speeds; the temporal and spatial variation in wind speed; the most frequent wind direction, also known as the prevailing wind direction; and the frequency of the remaining wind directions Manwell et al. (2002). The probability of the wind speed being above a given turbine rated wind speed can be used to predict how often the turbine operates in Region 3 at its maximum, that is, rated power capacity. The capacity factor CF is defined by the ratio:

$$CF = \frac{E_{out}}{E_{cap}} \quad (1)$$

where E_{out} is a wind turbine energy output over a period of time and E_{cap} is the energy the turbine would have produced if it had run at rated power for the same amount of time.

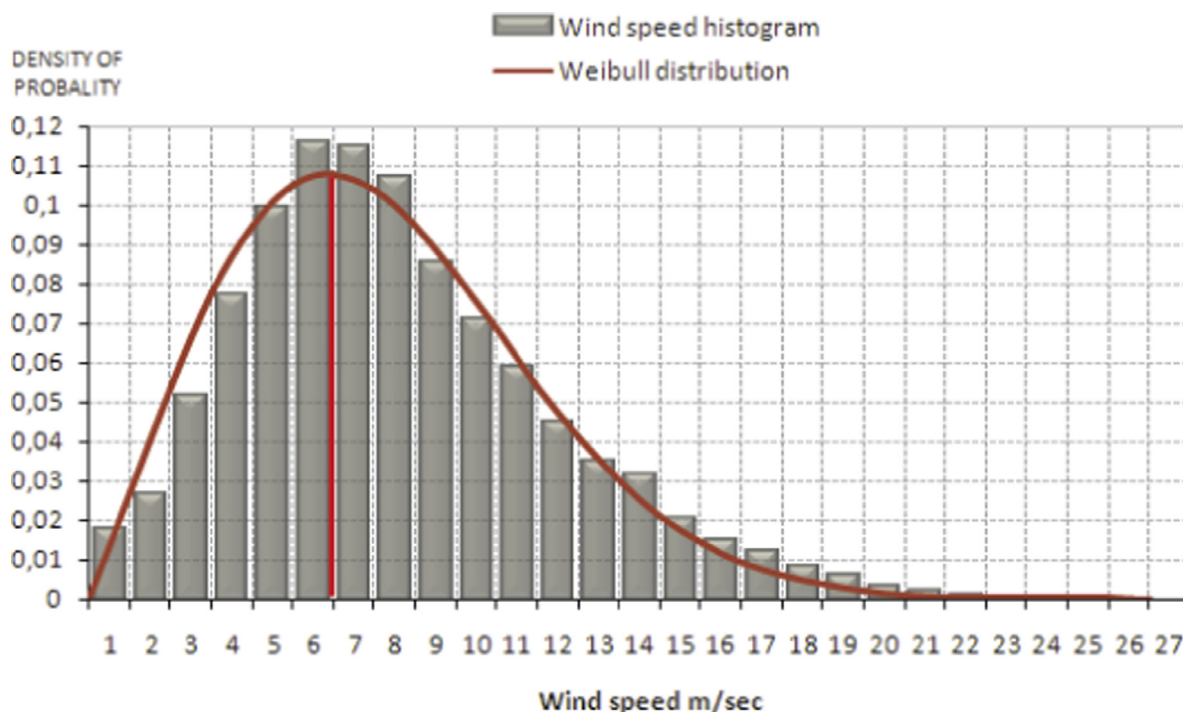


Fig. 6. Sample histogram of wind speed and Weibull function.

458 To predict the capacity factor and maintenance requirements for
 459 a wind turbine, it is useful to understand wind characteristics over
 460 both long and short time scales, ranging from multiyear to subsecond.
 461 Determining whether a location is suitable and economically advan-
 462 tageous for siting a wind turbine depends on the ability to measure
 463 and predict the available wind resource at that site. Significant varia-
 464 tions in seasonal average wind speeds affect a local area's available
 465 wind resource over the course of each year. Wind speed and direc-
 466 tion variations caused by the differential heating of the Earth's sur-
 467 face during the daily solar radiation cycle occur on a diurnal, that is,
 468 daily time scale. The ability to predict hourly wind speed variations
 469 can help utilities to plan their energy resource portfolio mix of wind
 470 energy and additional sources of energy. Finally, knowledge of short-
 471 term wind speed variations, such as gusts and turbulence, is used in
 472 both turbine and control design processes so that structural loading
 473 can be mitigated during these events.

474 Therefore, it is very important for the wind industry to be able
 475 to describe the variation of wind speeds. Turbine designers need the
 476 information to optimise the design of their turbines, so as to minimise
 477 generating costs. Turbine investors need the information to estimate
 478 their income from electricity generation.

479 If you measure wind speeds throughout a year, you will notice
 480 that in most areas strong gale force winds are rare, while moderate
 481 and fresh winds are quite common. The wind variation for a typical
 482 site is usually described using the Weibull distribution, as shown in
 483 Fig. 6. This particular site has a mean wind speed of 7 metres per sec-
 484 ond, and the shape of the curve is determined by a so-called shape
 485 parameter of 2.

486 Fig. 6 shows that 6.6 m/s is the median of the distribution, which is
 487 skewed, i.e. it is not symmetrical. Sometimes, very high wind speeds
 488 occur, but they are very rare. Wind speeds of 5.5 m/s, on the other
 489 hand, are the most common ones. 5.5 m/s is called the modal value of
 490 the distribution. The probability distribution function has the form of
 491 (2):

$$p(v) = \frac{k}{A} \left(\frac{v}{A}\right)^{k-1} e^{-\left(\frac{v}{A}\right)^k} \quad (2)$$

492 where $A > 0$ and $k > 0$ are the scale and shape parameters, respec-
 493 tively, which determine the function form. In particular, k determines
 494 the decrease rate of the function, whilst A represents the function
 495 skewness. Properly chosen parameters and a value for k indicates that
 496 the average speed and wind energy calculated from the gross Weibull
 497 distribution will be equal to that calculated from the histogram of the
 498 example in Fig. 6.

499 The statistical distribution of wind speeds varies from place to
 500 place around the globe, depending upon local climate conditions, the
 501 landscape, and its surface. The Weibull distribution may thus vary,
 502 both in its shape, and in its mean value. If the shape parameter is
 503 exactly 2, as in Fig. 6, the distribution is known as a Rayleigh distri-
 504 bution. Wind turbine manufacturers often give standard performance
 505 figures for their machines using the Rayleigh distribution.

506 It is worth noting that more detailed model of the wind are not
 507 usually exploited in the related literature, as shown for example in
 508 Odgaard et al. (2013), Odgaard and Stoustrup (2013), Odgaard and
 509 Stoustrup (0000). However, in the remainder of this section, a typical
 510 wind description is briefly outlined Burton et al. (2011). Wind can be
 511 modelled as the sum of a steady state mean wind and a perturbation
 512 wind, accounting for turbulence and/or gusts. The deterministic com-
 513 ponent of the wind field implements the transients specified by IEC
 514 61400-1 Bottasso, Croce, and Savini (2007), the exponential and log-
 515 arithmic wind shear models, and the tower shadow effects, which in-
 516 clude the potential flow model for a conical tower, the downwind em-
 517 pirical model Bottasso et al. (2007), or an interpolation of these two
 518 models. Their expressions will be omitted for brevity. The stochastic
 519 component of the wind field can be described according to the Von
 520 Karman or Kaimal turbulence models.

521 In this way, the wind model generates, from a scalar mean wind
 522 speed at hub height, a time-varying matrix that contains the wind
 523 speed for each point in the wind field:

$$V_{\text{field}}(t, R, \theta) = v_{\text{mean}}(t) + V_{\text{ws}}(t, R, \theta) + V_{\text{ts}}(t, R, \theta) + V_{\text{wk}}(t, R, \theta) \quad (3)$$

524 where V_{field} is the total wind speed field, v_{mean} is the mean wind
 525 speed, V_{ws} is the wind shear component, V_{ts} is the tower shadow

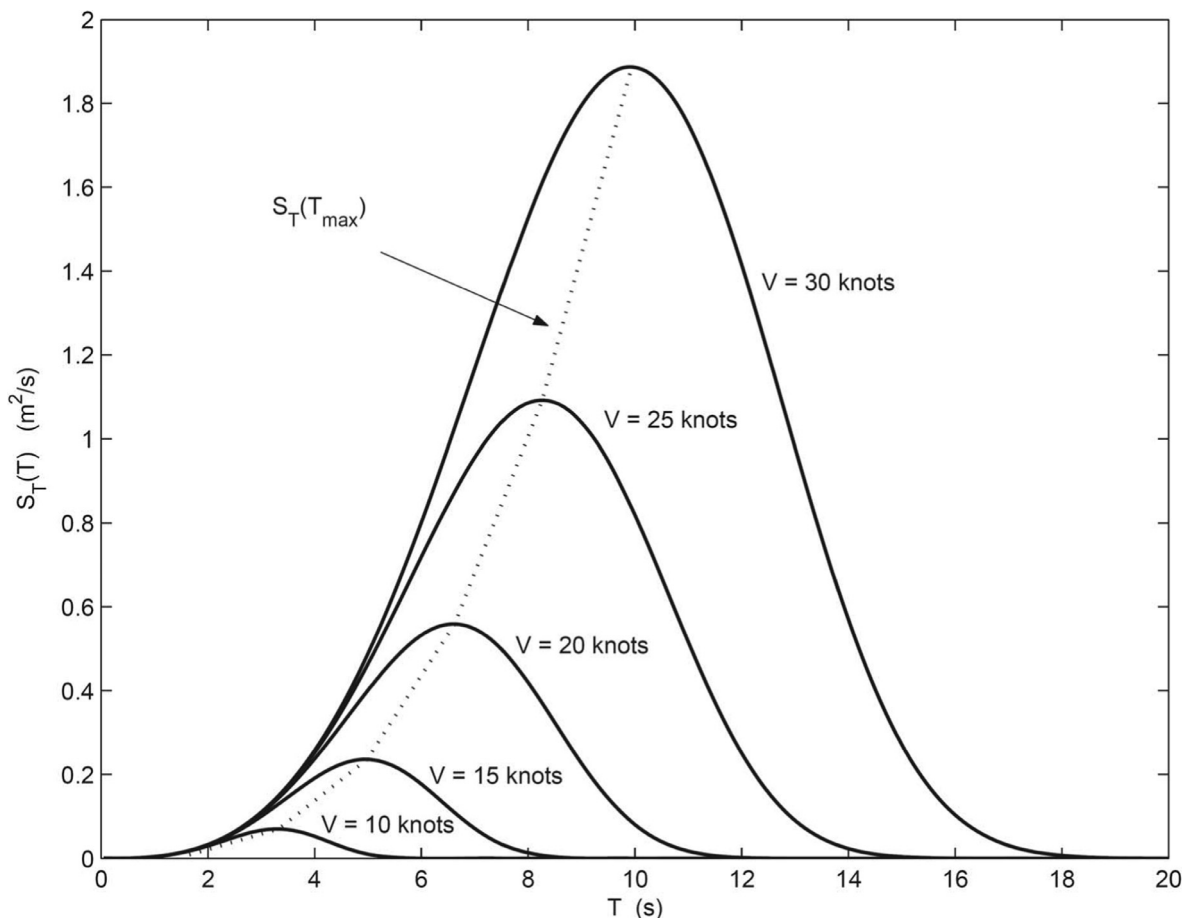


Fig. 7. Typical Pierson–Moskowitz wave spectra, from (5), for different steady-state wind velocities. Both the wave amplitude and period increase with an increase in the driving wind speed.

component, and V_{wk} is the far wake component of one preceding wind turbine (relevant for the case of wind farms). Notice the dependence on the rotor radius R , and rotor azimuth angle θ . When required, the simplified wake model is represented as a part of the wind field (i.e. a circle) with a lower wind speed Friis et al. (2011). The wake is centred around a point (R_0, φ) placed on the rim of the wind field, and with the form of (4):

$$R^2 - 2R R_0 \cos(\theta - \varphi) + R_0^2 = W^2 \quad (4)$$

where R_0 is the radial coordinate for the centre of the wake, φ is the angular coordinate of the centre of the wake, and W is the radius of the wake.

Finally, stochastic variables can be added to the wind components except tower shadow, giving a closer to reality parameterisation of the wind speeds throughout the rotor plane. In this way, the wind field is converted to equivalent winds signals that acts on two distinct parts of the blades, namely the tip and root sections, in order to obtain a linearisable model description.

2.2. Wave models

The two measurable properties of waves are height and period. Researchers and mariners usually characterise wave heights by the average of the highest one-third of the observed wave heights. This statistically averaged measure is termed the *significant wave height* and usually denoted as $H_{\frac{1}{3}}$ or H_s . In addition, real ocean waves do not generally occur at a single frequency. Rather, a distributed amplitude spectrum is used to model ocean waves, with random phases. Energy spectra are widely used to represent sea states Bretschneider (1952),

Pierson and Moskowitz (1964), Hasselmann (1973), Ochi (1998). A typical wave spectral density (or wave spectrum) has the form

$$S_T(T) = AT^3 e^{-BT^4}, \quad (5)$$

with the coefficients A and B , for example, given for the Pierson–Moskowitz model by Pierson and Moskowitz (1964) as

$$A = 8.10 \times 10^{-3} \frac{g^2}{(2\pi V)^4} \quad (6)$$

$$B = 0.74 \left(\frac{g}{2\pi V} \right)^4, \quad (7)$$

where V is the wind velocity measured 19.5 m above the Still-Water Level (SWL), g is the acceleration due to gravity, and T is the wave period in seconds. Some typical wave spectra generated from this model are shown in Fig. 7. Note that the available wave energy increases (approximately) exponentially with wave period T .

Not all waves are well represented by the spectral models of the type shown in (5). In some cases, where swell and local wind conditions are relatively uncorrelated (which can often be the case, for example, on the West Coast of Ireland International (2005)), ‘split spectra,’ consisting of spectra containing two distinct peaks, can occur. The variety of spectral shapes, some of which are illustrated in Fig. 8, presents a significant challenge to both the WEC designer and control engineer.

All of the aforementioned wave spectral models are for *fully developed waves*; in other words, the fetch (the distance over which the waves develop) and the duration for which the wind blows are sufficient for the waves to achieve their maximum energy for the given wind speed. In addition, linear wave theory is assumed, meaning that

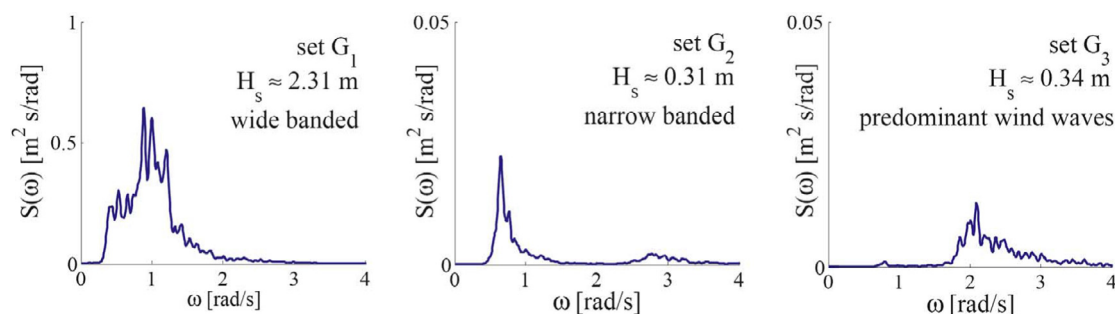


Fig. 8. Real wave spectra recorded at Galway Bay in Ireland. In general, low frequency waves have the highest power. Narrow-banded seas make wave forecasting and WEC control more straightforward, allowing a focus on a predominant single frequency.

574 waves are well represented by a sinusoidal form, which relies on the
575 assumption that there are no energy losses due to friction, turbu-
576 lence, or other factors, and that the wave height H is much smaller
577 than the wavelength λ .

578 However, not only is the ‘wind-wave’ component in Fig. 8 for set
579 G_3 at odds with the spectrum shown in Fig. 7, there are three distinct
580 low frequency components in set G_1 . Directional wave analysis
581 Gilloteaux and Ringwood (2009) can be used to reveal the
582 individual components. In general, with regard to wave directionality,
583 directional wave devices are tethered with nondirectional moorings,
584 which allow the devices to face the predominant wave direction
585 (weather vaning), or devices are nondirectional, such as heaving
586 buoy-type devices.

587 There are a number of exceptions to this general rule, including
588 shore-mounted oscillating water-column devices and, while many
589 devices can be considered nondirectional, the (fixed) moorings to
590 which they are attached are rarely truly nondirectional.

591 In general, a wave spectrum is assumed to be stationary for up to
592 3 h. Time–frequency analysis via the wavelet transform Nolan, Ring-
593 wood, and Holmes (2007) can be used to examine spectral variability.
594 For longer durations, such as a year, wave scatter diagrams (see
595 Fig. 9) provide a joint probability table of significant wave heights and
596 characteristic periods for a particular wave site. For example, the data
597 shown in Fig. 9 show two predominant wave climates which exist at
598 a particular site.

599 The energy in an ocean wave, consisting of both potential and
600 kinetic energy, is proportional to the square of the wave ampli-
601 tude McCormick (1981) and proportional to the wavelength,

$$E_w = E_p + E_k = \frac{\rho g H^2 \lambda b}{8}, \quad (8)$$

602 where H is the wave height above SWL, λ is the wavelength, ρ the
603 water density, and b the crest width. In deep water, the energy in
604 a linear wave is equally composed of potential energy (exhibited by
605 the wave height) and kinetic energy (dependent on the motion of the
606 particles), so that

$$E_p = E_k = \frac{\rho g H^2 \lambda b}{16}. \quad (9)$$

607 For simulation purposes, wave spectra are usually discretized and in-
608 dividual sinusoidal components used, where the amplitudes are de-
609 termined from the spectral density (such as in Fig. 7), and random
610 initial phases employed for the individual components.

611 2.3. Comparisons and contrasts of wave and wind model characteristics

612 The wind and wave models described in Sections 2.1 and 2.2 can
613 be used to evaluate how much the available raw power can be con-
614 verted into the actual extracted power from hypothetical wind and
615 wave farms. For example, regarding the power extracted from wind,
616 the relatively mature state of wind turbine technology permits the

617 use of well established power curves, and wind distribution func-
618 tions, as shown in Sections 2.1 and 3.2, respectively. Computing the
619 extracted power from wave energy devices, on the other hand, is not
620 quite as straightforward, mainly because of the fact that there is little
621 established commercial wave technology and the operating princi-
622 ples of the available devices are very diverse, so that it is difficult to
623 find a standardised measure of the extracted power. In addition, in-
624 stead of the single resource parameter (wind speed) in the case of
625 wind energy, a minimum of two parameters are needed to quantify
626 the wave power, from (8). This leads to the use, by some WEC devel-
627 opers, of the power matrix (for example in the case of the Pelamis
628 device), though some studies suggest that the two parameters usu-
629 ally used to model sea spectra (for example, as in (5)) are insufficient
630 to correctly detail power production capabilities De Andres, Guanche,
631 Vidal, and Losada (2015). This observation reflects that fact the oscil-
632 latory WECs, which make up the bulk of WEC types, are highly re-
633 sponsive to the spectral content of waves.

634 In order to determine the power extracted from wind or wave
635 farms, the power from single devices must be projected to the
636 corresponding number of wind turbines and wave energy converters.
637 Usually, the yearly average power output levels of the farms are
638 considered. The reason why the rated capacity is not used is that the
639 capacity factors for wind turbines and wave devices are not the same,
640 due to the significant differences in the probability distribution of
641 their produced power values. Wind turbines, most of the time, work
642 either at low level or at full capacity, whereas the wave power output
643 is mostly concentrated at average levels, so that a comparison based
644 solely on the capacity and not taking into account the capacity factor,
645 would be quite unjust and might return misleading results.

646 Moreover, the evaluation of the extracted power levels depend on
647 the particular device. In the case of wind, the well advanced state of
648 the technology resulted in a certain convergence of the performance
649 of the off-shore wind turbines available on the market, so that their
650 power curves are quite comparable. The field of wave energy, on the
651 other hand, is still an assortment of different devices, based on rather
652 diversified operating principles, so that their power characteristics
653 are very different and can also be very site specific.

654 One other contrast, between wind and wave systems, should be
655 noted in relation to resource quantification. For both wind and waves,
656 directionality plays an important role. However, while HAWTs can
657 yaw to face the wind, and VAWTs have no directional sensitivity
658 (though the site itself may be sensitive), many wave devices are
659 highly sensitive to wave direction. As already mentioned, though the
660 device itself (for example a point absorber) may be insensitive to
661 wave direction, the moorings which tether the device are not, leading
662 to a directional sensitivity.

663 3. Models for wind turbines and wave energy systems

664 In this section, the main models and their mathematical de-
665 scriptions for wind turbines and wave energy devices will be briefly

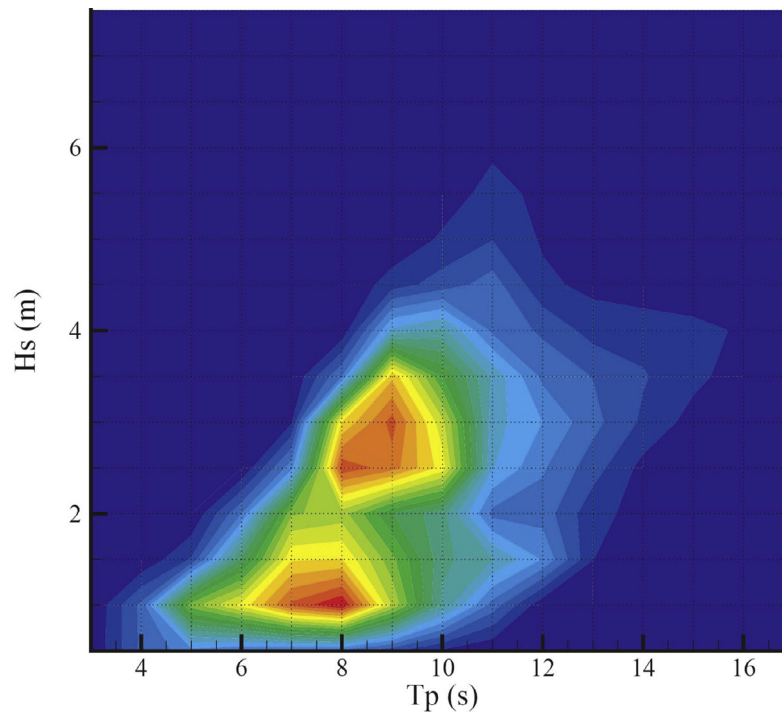


Fig. 9. Sample scatter diagram for the Atlantic Marine Energy Test Site (AMETS) at Belmullet, Ireland. In general, both peak period, T_p , and significant wave height, H_s , increase together. Typical Atlantic waves cover a period span of 6–12 s.

666 recalled, in order to highlight their main purpose oriented to the
667 design of control strategies.

668 3.1. Purposes of models

669 Prior to the design and application of new control strategies on
670 real wind turbines, the efficacy of the control scheme has to be tested
671 in detailed aero-elastic simulation model. Several simulation pack-
672 ages exist that are commonly used in academia and industry for wind
673 turbine load simulation. One of the most used simulation package is
674 the Fatigue, Aerodynamics, Structures, and Turbulence (FAST) code
675 [Jonkman and Buhl \(2005\)](#) provided by the National Renewable En-
676 ergy Laboratory (NREL) in Golden (Colorado, USA), since it represents
677 a reference simulation environment for the development of high-
678 fidelity wind turbine prototypes that are taken as a reference test-
679 cases for many practical studies [Jonkman, Butterfield, Musial, and](#)
680 [Scott \(2009\)](#). FAST provides a high-fidelity wind turbine model with
681 24 degrees of freedom, which is appropriate for testing the developed
682 control algorithms but not for control design. For the latter purpose,
683 a reduced-order dynamic wind turbine model, which captures only
684 dynamic effects directly influenced by the control, is recalled in this
685 section and it can be used for model-based control design [Bianchi](#)
686 [et al. \(2007\)](#). We can also note that the FAST tool has been evolved
687 to deal with wave energy devices and also complimented with the
688 WECSim tool, also developed by NREL.

689 The main issues used for highlighting similarities and differences
690 of the models that describe the behaviour of wind turbines and wave
691 energy devices will be articulated in the following.

692 3.2. Wind turbine models

693 Due to the competitive nature of the wind turbine industry and
694 possible confidentiality issues, the modelling available in the wind
695 turbine literature is usually kept at a conceptual level. For more de-
696 tailed modelling of pitch regulated wind turbines see, e.g., [Burton](#)
697 [et al. \(2011\)](#), [Muljadi and Butterfield \(1999\)](#), [Knudsen, Bak, and Soltani](#)
698 [\(2011\)](#). It is worth noting also that, in the wind turbine area, there

699 have been a number of IFAC and IEEE publications with sessions and
700 special issues starting from 2009, based also on competition studies,
701 e.g. [Ostergaard, Stoustrup, and Brath \(2009\)](#), [Pao and Johnson \(2011\)](#),
702 [Odgaard and Odgaard \(2012\)](#). These sessions and special issues have
703 led to important results and publications that will be briefly sum-
704 marised below, in order to give readers a basic research review.

705 Previous studies have shown that linear aero-elastic models used
706 for the analysis of wind turbines are commonly of very high order.
707 Multibody dynamics coupled with unsteady aerodynamics (e.g. dy-
708 namic stall) are among the recently developments in wind turbine
709 aero-elasticity [Rasmussen et al. \(2003\)](#), [Bianchi et al. \(2007\)](#), [Hansen](#)
710 [\(2011\)](#). The resulting models contains hundreds or even thousands
711 of flexible modes and aerodynamic delays. In order to synthesise
712 wind turbine controllers, a common practice is to obtain linear time-
713 invariant (LTI) models from a nonlinear model for different operating
714 points. Modern control analysis and synthesis tools are inefficient for
715 such high-order dynamical systems; reducing the model size is crucial
716 to analyse and synthesise model-based controllers. The most inter-
717 esting solution available in the literature relies on the Linear Parameter
718 Varying (LPV) framework, as it has shown to be
719 suitable to cope, in a systematic manner, with the inherent varying
720 dynamics of a wind turbine over the operating envelope [Bianchi et al.](#)
721 [\(2007\)](#), [Ostergaard et al. \(2009\)](#), [Adegas, Sloth, and Stoustrup \(2012\)](#),
722 [Adegas, Sonderby, Hansen, and Stoustrup \(2013\)](#). Wind turbine LPV
723 models are usually simple, first-principles based, often neglecting
724 dynamics related to aerodynamic phenomena and some structural
725 modes. This in turn restricted LPV control of wind turbines to the
726 academic environment only. A procedure to encapsulate high-fidelity
727 dynamics of wind turbines as an LPV system would be beneficial to
728 facilitate industrial use of LPV control.

729 Other modelling approached that one may find in the literature
730 are based on some type of simplified wind turbine descriptions
731 [Pedersen and Fossen \(2012\)](#). These may have the form of lookup-
732 tables as in [Bianchi et al. \(2007\)](#) or linear models obtained from
733 complex numerical simulation tools [Namik and Stol \(2010\)](#). Hybrid
734 models blending lookup tables with mechanical models have also
735 been used [Bottasso et al. \(2007\)](#). These and even simpler approaches

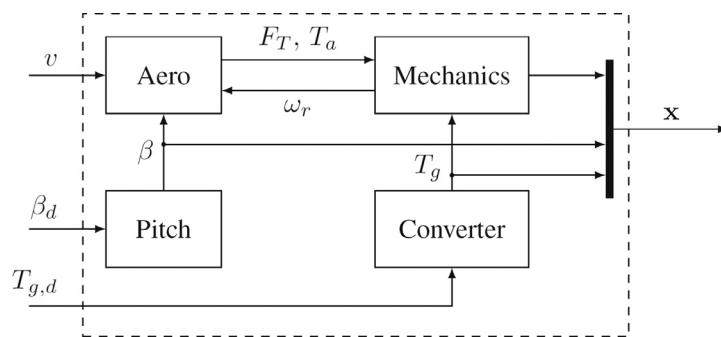


Fig. 10. Block diagram of the complete wind turbine model.

736 predominate. Linear models can be valid in a small envelope around
737 the linearisation point, which requires several individual models to
738 cover the operational domain of the turbine [Pintea, Popescu, and](#)
739 [Borne \(2010\)](#).

740 However, most of the control algorithms for modern variable-
741 pitch wind turbines, that one may find in the literature, are usually
742 based on some type of simplified wind turbine linear model. There-
743 fore, after these considerations, this section will address the most im-
744 portant components of a HAWT used for the linear modelling of a
745 wind turbine installation. They consist of the wind turbine tower, its
746 nacelle, and the rotor, visible from the ground, as depicted in [Fig. 1](#).

747 As sketched in [Fig. 10](#), the complete wind turbine model consists
748 of several submodels for the mechanical structure ('Mechanics'), the
749 aerodynamics ('Aero'), as well as the dynamics of the pitch system
750 ('pitch') and the generator/converter system ('converter'). The gen-
751 erator/converter dynamics are usually described as a first order delay
752 system. However, when the delay time constant is very small, an ideal
753 converter can be assumed, such that the reference generator torque
754 signal is equal to the actual generator torque. In this situation, the
755 generator torque can be considered as a system input, whilst the gen-
756 erator is the device that converts mechanical energy from the aero-
757 dynamic torque to electrical energy.

758 [Fig. 10](#) reports also the wind turbine inputs and outputs. In partic-
759 ular, v is wind speed, F_T and T_a correspond to the rotor thrust force
760 and rotor torque, respectively; ω_r is the rotor angular velocity, x the
761 state vector, T_g the generator torque, and $T_{g,d}$ the demanded gener-
762 ator torque. β is the pitch angle, whilst β_d its demanded value.

763 The drive-train, consisting of rotor, shaft and generator is mod-
764 elled as a two-mass inertia system, including the shaft torsion θ_Δ ,
765 where the two inertias are connected with a torsional spring with
766 spring constant k_S and a torsional damper with damping constant d_S .
767 The angular velocities ω_r and ω_g are the time derivatives of the ro-
768 tation angles θ_r and θ_g . The drive-train can be thus described as the
769 following linear system:

$$\begin{bmatrix} \dot{\omega}_r(t) \\ \dot{\omega}_g(t) \\ \dot{\theta}_\Delta(t) \end{bmatrix} = \begin{bmatrix} -\frac{B_S + B_r}{J_r} & \frac{B_S}{n_g J_r} & -\frac{k_S}{J_r} \\ \frac{\eta_{dt} B_S}{n_g J_g} & -\frac{\eta_S B_S}{n_g^2} - B_g & \frac{\eta_S k_S}{n_g J_g} \\ 1 & -\frac{1}{n_g} & 0 \end{bmatrix} \begin{bmatrix} \omega_r(t) \\ \omega_g(t) \\ \theta_\Delta(t) \end{bmatrix} + \begin{bmatrix} \frac{1}{J_r} & 0 \\ 0 & -\frac{1}{J_g} \\ 0 & 0 \end{bmatrix} \begin{bmatrix} T_a \\ T_g \end{bmatrix} \quad (10)$$

770 where J_r is the moment of inertia of the low speed shaft (rotor), B_g
771 is the viscous friction of the high speed shaft (generator), J_g is the

772 moment of inertia of the high speed shaft, and η_{dt} is the efficiency
773 of the drive train. The rotor torque T_a is generated by the lift forces
774 on the individual blade elements, whilst T_g represents the generator
775 torque. The ideal gearbox effect can be simply included in the gener-
776 ator model by multiplying the generator inertia J_g by the square of the
777 gearbox ratio n_g .

778 In pitch-regulated wind turbines, the pitch angle of the blades is
779 controlled only in the full load region to reduce the aerodynamic rotor
780 torque, thus maintaining the turbine at the desired rotor speed.
781 Moreover, the pitching of the blades to feather position (*i.e.* 90°) is
782 used as main braking system to bring the turbine to standstill in crit-
783 ical situations. Two different types of pitch technologies are usually
784 exploited in wind turbines, *i.e.* hydraulic and electromechanical pitch
785 systems. For hydraulic pitch systems, the dynamics can be modelled
786 by means of a second-order dynamic model [Odgaard et al. \(2013\)](#),
787 which is able to display oscillatory behaviour. For electromechanical
788 pitch systems, which are more commonly used, a first-order delay
789 model is sufficient. In this work, the first-order delay model is
790 recalled:

$$\dot{\beta} = -\frac{1}{\tau} \beta + \frac{1}{\tau} \beta_d \quad (11)$$

791 where β and β_d are the physical and the demanded pitch angle, re-
792 spectively. The parameter τ denotes the time constant.

793 An explicit model for the generator/converter dynamics can be in-
794 cluded into the complete wind turbine system description. Note that
795 for mere simulation purposes, this is not necessary, since the gener-
796 ator/converter dynamics are relatively fast. However, when advanced
797 control designs are considered, an explicit generator/converter model
798 might be required in order to take into account the fast generator
799 torque dynamics. In this case, a simple first order dynamic model can
800 be sufficient, as described *e.g.* in [Odgaard et al. \(2013\)](#):

$$\dot{T}_g = -\frac{1}{\tau_g} T_g + \frac{1}{\tau_g} T_{g,d} \quad (12)$$

801 where $T_{g,d}$ represents the demanded generator torque, whilst τ_g the
802 delay time constant.

803 The aerodynamic submodel consists of the expressions for the
804 thrust force F_T acting on the rotor and the aerodynamic rotor torque
805 T_a . They are determined by the reference force F_{st} and by the aero-
806 dynamic rotor thrust and torque coefficients C_T and C_Q [Gasch and Tvele](#)
807 [\(2012\)](#):

$$\begin{cases} F_T = F_{st} C_T(\lambda, \beta) \\ T_a = F_{st} R C_Q(\lambda, \beta) \end{cases} \quad (13)$$

808 The reference force F_{st} is defined from the impact pressure $\frac{1}{2} \rho v^2$ and
809 the rotor swept area πR^2 (with rotor radius R), where ρ denotes the
810 air density:

$$F_{st} = \frac{1}{2} \rho \pi R^2 v^2 \quad (14)$$

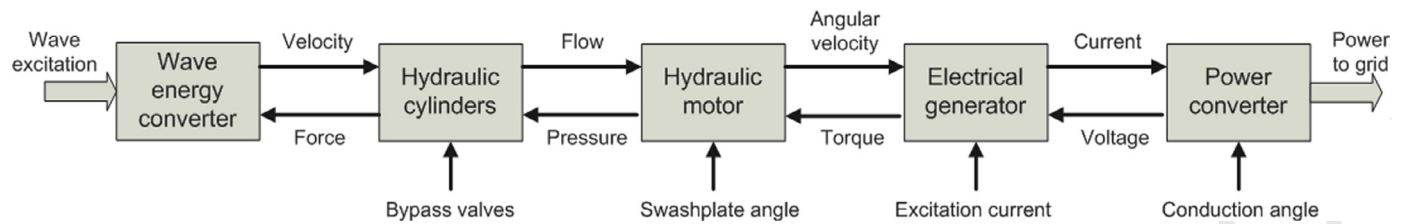


Fig. 11. Wave-energy PTO system components and potential control inputs. In general, only one of these control inputs is used by the energy-maximising control.

811 It is worth noting that, for simulation purposes, the static wind speed
812 v is used. The aerodynamic maps C_T and C_Q used for the calcula-
813 tion of the rotor thrust and torque are usually represented as static
814 2-dimensional tables, which already take into account the dynamic
815 contributions of both the tower and the blade motions.

816 As highlighted in the expressions (13), the rotor thrust and torque
817 coefficients (C_T, C_Q) depend on the tip speed ratio $\lambda = \frac{\omega_r R}{v}$ and the
818 pitch angle β . Therefore, the rotor thrust F_T and torque T_a assume the
819 following expressions:

$$\begin{cases} F_T = \frac{1}{2} \rho \pi R^2 C_T(\lambda, \beta) v^2 \\ T_a = \frac{1}{2} \rho \pi R^3 C_Q(\lambda, \beta) v^2 \end{cases} \quad (15)$$

820 Note that the rotor thrust in (13) and (15) is a horizontal force,
821 i.e. a structural load, which should be mitigated, as suggested in
822 Section 4.2 Bossanyi (2003).

823 The expressions (15) highlight that the rotor thrust F_T and torque
824 T_a are nonlinear functions dependent on the wind speed v , the ro-
825 tor speed ω_r , and the pitch angle β . These functions are usually ex-
826 pressed as two-dimensional maps, which must be known for the
827 whole range of variation of both the pitch angles and tip speed ra-
828 tios. These maps are usually a static approximation of more detailed
829 aerodynamic computations that can be obtained using, for example,
830 the Blade Element Momentum (BEM) method. In this case, the aero-
831 dynamic lift and drag forces at each blade section are calculated and
832 integrated in order to obtain the rotor thrust and torque Gasch and
833 Tvele (2012). More accurate maps can be obtained by exploiting the
834 calculations implemented via the AeroDyn module of the FAST code,
835 where the maps are extracted from several simulation runs Laino and
836 Hansen (2002).

837 It is worth noting that for simulation purposes, the tabulated ver-
838 sions of the aerodynamic maps C_Q and C_T are sufficient. On the other
839 hand, for control design, the derivatives of the rotor torque (and
840 thrust) are needed, thus requiring a description of the aerodynamic
841 maps as analytical functions. Therefore, these maps can be approxi-
842 mated using combinations of polynomial and exponential functions,
843 whose powers and coefficients are estimated via e.g. modelling Heir
844 (2014) or identification Simani and Castaldi (2014) approaches.

845 Wind turbine high-fidelity simulators, which were described for
846 example in Odgaard and Johnson (2013), consider white noise added
847 to all measurements. This relies on the assumption that noisy sensor
848 signals should represent more realistic scenarios. However, this is not
849 the case, as a realistic simulation would require an accurate knowl-
850 edge of each sensor and its measurement reliability. To the best of
851 the authors' knowledge, all main measurements acquired from the
852 wind turbine process (rotor and generator speed, pitch angle, gener-
853 ator torque), are virtually noise-free or affected by very weak noise.

854 3.3. Wave energy device models

855 Since PTO systems for wave energy converters are quite non-
856 standard, the focus here will be on the hydrodynamic part of the WEC
857 model, though modelling aspects concerning the generator/converter
858 system from Section 3.2 are also relevant.

Mathematical models of wave-energy devices, as in the wind en- 859
ergy case, are required for a variety of purposes: 860

- 861 1. Assessment of power production 861
- 862 2. Assessment of loading forces under extreme sea conditions 862
- 863 3. Simulation of device motion, including evaluating the effective- 863
ness of control strategies 864
- 865 4. For use as a basis for model-based control design. 865

866 Mathematical models for wave-energy devices should, ideally, 866
encompass the water/device (hydrodynamic) interactions and the 867
PTO system, and may also include a model for connection to an 868
electrical grid, thus presenting a total 'wave-to-wire' model Josset, 869
Babarit, and Clement (2007). While the PTO and grid (or possibly 870
other downstream energy consumers, such as reverse osmosis units) 871
may be modelled using more traditional physical lumped-parameter 872
modelling methodologies, the determination of the hydrodynamic 873
model for a WEC, or array of WECs, is nontrivial. A variety of mod- 874
elling methodologies are available, most of which involve the solution 875
to partial differential equations across a numerical mesh. 876

877 Among the possible hydrodynamic solvers with the highest fi- 877
delity are algorithms based on smooth particle hydrodynamics (SPH) 878
Cleary, Prakash, Ha, Stokes, and Scott (2007) or computational fluid 879
dynamics (CFD) Agamloh, Wallace, and von Jouanne (2008). Such 880
approaches can articulate the full range of nonlinear hydrodynamic 881
forces in three dimensions. However, given the significant computa- 882
tional overhead of such approaches (typically a second of simulation 883
time takes around an hour of computation time), they are not ideal 884
either as a basis for model-based control design, nor as a simulation 885
tool to evaluate the effectiveness of various control designs. However, 886
CFD models have been used to develop simpler parametric models, 887
which can provide a basis for control design and simulation Davidson, 888
Giorgi, and Ringwood (2013). 889

890 The remainder of this section is primarily devoted to the develop- 890
ment of hydrodynamic models. An outline of a possible PTO system 891
is shown in Fig. 11, and shows the possible inclusion of mechanical, 892
hydraulic, and electrical components. In many cases, for example for 893
the SeaBased device Trapanese (2008), the WEC is directly coupled 894
to a linear generator, eliminating the hydraulic components. Given the 895
many potential changes of energy form evident from Fig. 11, bond 896
graphs have been shown to be a powerful tool in providing a sys- 897
tematic graphical procedure to determine mathematical models for 898
wave-energy PTO systems Bacelli, Gilloteaux, and Ringwood (2008), 899
or complete wave-energy systems Hals (2010). 900

901 3.3.1. Linear models and cummins' equation 901

902 Consider a single-body floating system oscillating in heave, 902
schematically depicted in Fig. 12. Energy is extracted from the relative 903
motion with the sea bottom, through a generic PTO mechanism. The 904
external forces acting on the WEC are the excitation from the waves 905
and the control force produced by the PTO, namely $f_{ex}(t)$ and $f_u(t)$. 906
Additional hydrodynamic and hydrostatic forces, which arise due to 907
the motion of the body in the water, are the radiation force $f_r(t)$, the 908
diffraction force $f_d(t)$, the viscous force $f_v(t)$, and the buoyancy force 909
 $f_b(t)$ Falnes (2002). 910

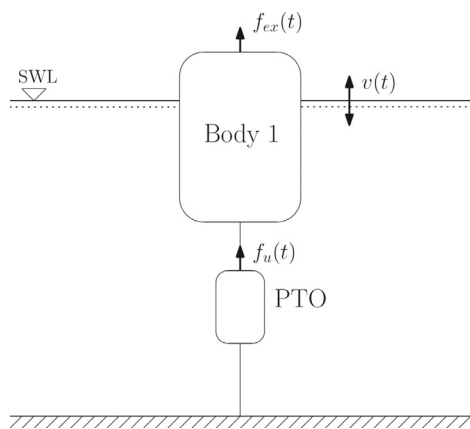


Fig. 12. One-degree-of-freedom floating system for wave-energy conversion. The lower side of the PTO is anchored to the sea bed, which provides an absolute reference for device motion.

911 The radiation force $f_r(t)$ is a damping/inertial force associated due
 912 to the fact that device motion, resulting in the production of radi-
 913 ated waves, is affected by the surrounding fluid. Such radiation forces
 914 are present even in the absence of incident waves and can be esti-
 915 mated using free response tests. The diffraction (or scattering) force
 916 $f_d(t)$ describes the force experienced by the device when scattering
 917 incident waves, and is independent of the device motion. The viscous
 918 damping force $f_v(t)$ is a nonlinear force, and becomes significant with
 919 increased device velocity. It is particularly relevant where the body
 920 surface contains discontinuities (such as flanges), which result in the
 921 creation of vortices. Finally, the buoyancy force is related to the de-
 922 flection of the device from its equilibrium (still water) position and
 923 is a balance between the Archimedes buoyancy force and the gravity
 924 force.

925 The equation of motion, following Newton’s second law and
 926 where a superposition of forces is assumed, in one degree of freedom
 927 is:

$$M\dot{v}(t) = f_m(t) + f_r(t) + f_d(t) + f_v(t) + f_b(t) + f_{ex}(t) + f_u(t) \quad (16)$$

928 where $v(t)$ is the heaving velocity and M is the WEC mass.

929 With the assumptions associated with linear potential theory
 930 Falnes (2002), namely that the fluid is irrotational, incompressible,
 931 and inviscid; the WEC body has a small cross-sectional area (or equiv-
 932 alently, the wave elevation is constant across the whole body); and
 933 the body experiences small oscillations (so that the wetted surface
 934 area is nearly constant); the equation of motion simplifies to

$$f_{ex} + f_d(t) = \int_{-\infty}^{+\infty} h_{ex}(\tau)\eta(t - \tau)d\tau \quad (17)$$

$$f_r(t) = -\int_0^t h_r(\tau)v(t - \tau)d\tau - m_\infty\dot{v}(t) \quad (18)$$

$$f_b(t) = -\rho g S_w \int_0^t v(\tau)d\tau = -K_b x(t) \quad (19)$$

$$f_v(t) = 0 \quad (20)$$

938 In (17), the excitation (and diffraction) force is related to the in-
 939 cident wave free surface elevation $\eta(t)$ through the excitation kernel
 940 function $h_{ex}(t)$. The expression (18) expresses the radiation force as a
 941 linear convolution of the radiation kernel $h_r(t)$ with the device oscil-
 942 lation velocity $v(t)$. Note that $h_{ex}(t)$ and $h_r(t)$ effectively describe the
 943 impulse responses in excitation force and radiation force to impulses
 944 in free surface elevation and device motion, respectively. Added mass,
 945 denoted by m_∞ in (18), reflects an effective increase in the device in-
 946 ertia since an accelerating floating body moves some volume of the
 947 surrounding fluid. In general, added mass is a frequency-dependent

quantity but is often approximated by its infinite frequency asymp-
 948 tote m_∞ .

949 The buoyancy force $f_b(t)$ in (19) models the hydrostatic equilib-
 950 rium, related to the heaving position through a linear coefficient that
 951 depends on the gravity acceleration g , the water density ρ , and the
 952 surface area of the body cut by the mean water level S_w . Note the
 953 noncausality of the expression for the excitation force in (17), where
 954 $h_{ex}(t) \neq 0$ for $t \leq 0$ Falnes (2002). The expression in (16), excluding
 955 the mooring force $f_m(t)$ and the viscous damping force $f_v(t)$ results in
 956 the widely used Cummins’ equation Cummins (1962):
 957

$$(M + m_\infty)\dot{v}(t) + \int_0^{+\infty} h_r(\tau)v(t - \tau)d\tau + K_b x(t) = \int_{-\infty}^t h_{ex}(\tau)\eta(t - \tau)d\tau. \quad (21)$$

958 which provides a linear integro-differential model for the motion of a
 959 WEC in response to variation in free-surface elevation $\eta(t)$, excluding
 960 the applied resisting PTO force, $f_u(t)$.

961 To focus on the control problem, the mooring force $f_m(t)$ is omitted
 962 from the following analysis, while the viscous damping force $f_v(t)$ is
 963 discussed in the next subsection. Typically, $h_{ex}(t)$ and $h_r(t)$ are calcu-
 964 lated numerically using boundary-element potential methods such
 965 as WAMIT WAMIT (2002), which performs the calculations in the
 966 frequency domain, or ACHIL3D Clement (2009), where time-domain
 967 calculations are used. The relation (21) can also be used to model
 968 multibody systems Bacelli and Ringwood (2013c) or arrays of devices
 969 Bacelli and Ringwood (2013b), with the modification that M , m_∞ , K ,
 970 and the hydrodynamic parameters represented by $h_{ex}(t)$ and $h_r(t)$, all
 971 increase in dimension accordingly.

3.3.2. Radiation damping approximations

972 Typically, for both simulation and control applications, the radia-
 973 tion damping convolution term in (18) is replaced by a closed form
 974 (finite order) equivalent. This replacement has several advantages.
 975 The integro-differential equation in (21) is replaced by a higher order
 976 differential equation, making analysis more straightforward, the
 977 resulting finite-order dynamical system is faster to simulate, and the
 978 closed-form dynamical equation can be used as a basis for model-
 979 based control design.

980 In general, $h_r(t)$ (and its Fourier transform, $H_r(\omega)$) are nonpara-
 981 metric in form, being the result of a numerical calculation on a
 982 distributed system. Approximations can be determined in either
 983 the time or frequency domain, depending on the manner in which
 984 $h_r(t) \leftrightarrow H_r(\omega)$ was determined, and the intended (time/frequency do-
 985 main) use of the finite-order approximation. For example, WAMIT
 986 (2002) uses a frequency-domain analysis to determine $H_r(\omega)$ di-
 987 rectly and approximations based on WAMIT data are usually based
 988 on frequency-domain error criteria. In such a case, state-space forms
 989 Perez and Fossen (2007) or transfer function forms McCabe, Brad-
 990 shaw, and Widden (2005) may be determined using frequency-
 991 domain identification Levy (1959).
 992

993 Alternatively, if $h_r(t)$ is directly produced, for example from a
 994 time-domain code such as ACHIL3D Clement (2009), time-domain
 995 impulse-response fitting can be employed, typically using the
 996 method in Prony (1795). In general, an order 4–10 linear approxima-
 997 tion to $h_r(t)$ is used, for both time- and frequency-domain approaches.
 998 In some cases a second-order approximation is adequate and has the
 999 added advantage of giving a pole pair, which has a strong connection
 1000 with the radiation damping transient response. Taghipour, Perez, and
 1001 Moan (2008) provides an overview of, and background to, the calcula-
 1002 tions of finite-order approximations to $h_r(t) \leftrightarrow H_r(\omega)$. Taghipour et al.
 1003 (2008) also considers finite-order approximation to the excitation
 1004 force kernel $h_{ex}(t)$ (with Fourier transform $F_{ex}(\omega)$), as does McCabe
 1005 et al. (2005).

3.4. Comparison of wind and wave device models

There is a stark contrast in the modelling focus within the wind and wave communities. For wind turbines, the static relationship between the optimal rotation speed, pitch angle and incident wind speed is well understood and is enumerated for each wind turbine. In the wave energy case, there is a complex dynamic relationship between the free surface elevation and the device motion. As a result, models for wind turbines focus more on the turbine mechanics, rather than the aerodynamics. In the wave energy case, considerable effort is expended on accurately modelling the hydrodynamics of the system and, in contrast, there are a relatively small amount of studies with modelling the PTO section, which forms part of the lower control loop in Fig. 5. No doubt, one of the reasons for such a lack of generic PTO models is the lack of convergence or standardisation of PTO systems for wave energy devices, which may be appreciated from the possibilities articulated in Fig. 11. In addition, few devices have reached the stage of full scale prototype and, in many of those cases, most attention is focussed on the physical (device and PTO) design, with the control aspects receiving secondary attention.

On notable comparative feature, but contrasting in specific number, is the overall theoretical maximum percentage of energy which can be usefully converted from wind and wave systems. The well-known Betz limit [Betz and Randall \(1966\)](#) for wind turbines, which limits the converted power to 60%, contrasts with the 50%, obtained under optimal control conditions (shown in [Section 4.3 Falnes \(2002\)](#)) for wave energy devices.

4. Control strategies

While [Section 3](#) focusses mainly on energy conversion system modelling and [Section 1](#) has recalled the classical control problem of regulation of some variable to a desired value, and indeed such problems are encountered in both wind and ocean energy applications, there is a broader set of problems which can also be addressed by control system technology. The purpose of this section is to present this broad problem definition and examine how this problem may be addressed, or broken down into smaller parts which may be more easily solved.

4.1. Background to strategy development (objectives and available tools)

In the case of both wind and wave energy, the general problem is to maximise energy capture, subject to grid and environmental constraints. However, we might modify the objective of energy capture maximisation to that of maximisation of economic return [Costello, Teillant, and Ringwood \(2012\)](#), which requires a balance to be achieved between maximising energy capture and minimising wear on components. However, the move to an economic performance function also requires the accurate articulation of capital and operational costs, which is quite onerous for the relatively immature field of ocean energy, and significantly complicates the optimisation problem. Instead, for the current analysis, in order to retain a focus on the fundamental control issues, this section is focussed on the problem of energy capture maximisation.

There are two broad approaches, which may be taken to solve the energy maximisation problem:

1. Overall extremum seeking control [Pao and Johnson \(2011\)](#), with little use of a detailed model of the system;
2. Determination of an optimal setpoint for the system, which gives maximum energy capture, followed by a regulator to make sure this setpoint is achieved [Bossanyi and Hassan \(2000\)](#).

Approach 1 is attractive from the point of view of the lack of requirement for a detailed model, but may have dynamic performance

limitations in convergence rates and may have difficulty finding a global maximum over a non-convex performance surface. For example, in wind turbines, this issue is important when the system is working below the rated wind speed, as recalled in [Section 4.2](#). On the other hand, in a wave energy application, the controller may not converge to the appropriate setting before the instantaneous wave frequency changes.

Interestingly, a common framework for both wind and wave energy may be adopted for the item 2, as shown in [Fig. 5](#). The particulars for wind and wave control solutions are detailed in [Sections 4.2 and 4.3](#), respectively. For the standard feedback regulation part of [Fig. 5](#), any one of the techniques mentioned in [Section 1](#) can be chosen, based on the particular system description, the level of control fidelity required and the appetite for computational complexity. Since both wind turbine and wave energy device dynamics are relatively slow (with the possible exception of the electronic power converter section), there is much scope for the implementation of complex control strategies.

4.2. Control strategies for wind turbines

In the case of a wind turbine, optimal blade pitch, β , and rotor velocity (via the tip/speed ratio, λ) are set based on the incident wind flow velocity, in order to maximise the power coefficient, C_Q . The manipulated variable for the pitch control is the power to the pitch actuators (voltage and/or current). For torque control, the generator excitation is used as a control actuator. It is worth noting that the relationship between β , λ , and C_Q is specific to each wind turbine, and must be determined for each particular case. However, this relationship is then fixed, though some slight variation may occur due, for example, to component wear or installation errors. Note also that when a wind turbine reaches its rated power (*i.e.* above the rated wind speed), the turbine needs to be 'depowered' in order to avoid exceeding any rated specifications. In this situation, it is not required to maximise power conversion (*i.e.* the wind power that can be converted into electric energy) and, for variable pitch turbines, blade pitch can be adjusted in order to limit power converted.

As already remarked in [Section 3.2](#), in the wind area there have been a number of IFAC and IEEE publications, sessions and special issues starting from 2011, based also on competition studies, addressing basic and advanced wind turbine control issues, *e.g.* [Odgaard and Stoustrup \(2011\)](#), [Diaz-Guerra, Adegas, and Stoustrup \(2012\)](#), [Biegel, Madjidian, Spudic, Rantzer, and Stoustrup \(2013\)](#), [Pao and Johnson \(2011\)](#), [Adegas and Stoustrup \(2012\)](#), [Odgaard and Odgaard \(2012\)](#).

On the other hand, previous investigations *e.g.* [Muljadi and Butterfield \(1999\)](#), [Leithead and Connor \(2000\)](#), [Bossanyi and Hassan \(2000\)](#), [Bianchi et al. \(2007\)](#) have shown that linear, time-invariant methods provide good closed-loop results when observing local behaviour. A natural choice for controller design covering the entire operating envelope is therefore to design linear controllers along a chosen operating trajectory and then to interconnect them in an appropriate way in order to get a control formulation for the entire operating region. This approach is denoted as gain scheduling and in [Cutululis, Ceanga, Hansen, and Sorensen \(2006\)](#) this is done by interpolating the outputs of a set of local controllers (either by linear interpolation or by switching). Alternatively, parameters of the controller are updated according to a pre-specified function of a measured/estimated variable [Leithead and Connor \(2000\)](#). A systematic way of designing such parameter-dependent controllers is within the framework of LPV systems, already recalled in [Section 3.2](#). In this case, the model is represented by a linear model at all operating conditions and a controller with similar parameter dependency is synthesised to guarantee a certain performance specification for all possible parameter values within a specified set. A major difference to classical gain scheduling is that it is possible to take into account that the scheduling parameters can vary in time

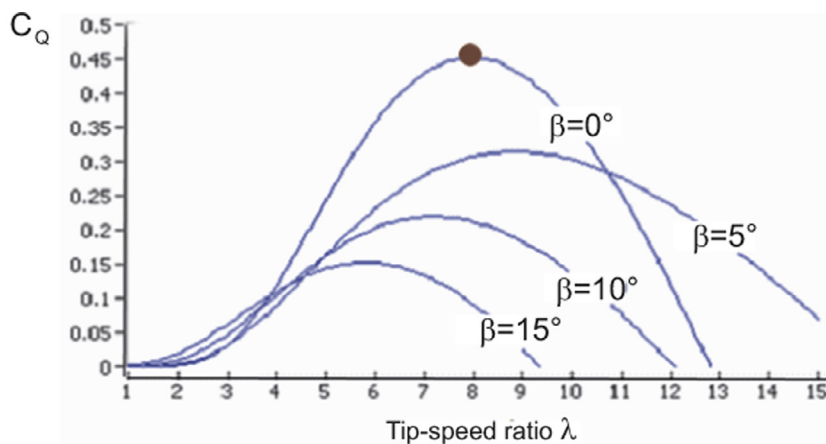


Fig. 13. Example of power coefficient curve.

1130 Ostergaard et al. (2009). Other controllers with different structures,
1131 e.g. linear quadratic, and repetitive model predictive, to mention a
1132 few more Adegas and Stoustrup (2012), Diaz-Guerra et al. (2012),
1133 Adegas and Stoustrup (2011), were also designed and applied to wind
1134 turbine systems.

1135 After these considerations, control systems for wind turbines
1136 seem now well developed Bianchi et al. (2007) and the fundamental
1137 control strategies are sketched below, in order to provide the readers
1138 a basic research review.

1139 The primary Region 2 control objective for a variable-speed wind
1140 turbine is to maximise the power coefficient, and in particular the C_Q
1141 map in (13). The relationship between C_Q and the tip-speed ratio λ is
1142 a turbine-specific nonlinear function. C_Q also depends on the blade
1143 pitch angle in a nonlinear way, and these relationships have the same
1144 basic shape for most modern wind turbines. An example of C_Q surface
1145 is shown in Fig. 13 for a generic wind turbine.

1146 As shown in Fig. 13, the turbine will operate at its highest aerody-
1147 namic efficiency point, C_{max} , at a certain pitch angle and tip-speed ra-
1148 tio. The pitch angle is easy to control, and can be reliably maintained
1149 at the optimal efficiency point. However, the tip-speed ratio depends
1150 on the incoming wind speed v and therefore is constantly changing.
1151 Thus, the Region 2 control is primarily concerned with varying the
1152 turbine speed to track the wind speed. When this approach is used,
1153 the controller structure for partial load operation follows the sequen-
1154 tial optimal calculation and regulation shown in Fig. 5.

1155 On utility-scale wind turbines, Region 3 control is typically per-
1156 formed via a separate pitch control loop. In the Region 3, the pri-
1157 mary objective is to limit the turbine power so that safe electrical
1158 and mechanical loads are not exceeded. Power limitation is achieved
1159 by pitching the blades or by yawing the turbine out of the wind, both
1160 of which can reduce the aerodynamic torque below what is theoret-
1161 ically available from an increase in wind speed. In the Region 3, the
1162 pitch control loop regulates the rotor speed ω_r (at the turbine 'rated
1163 speed') so that the turbine operates at its rated power.

1164 In this way, the overall strategy of the wind turbine controller is
1165 to use two different controllers for the partial load region and the
1166 full load region. When the wind speed is below the rated value, the
1167 control system should maintain the pitch angle at its optimal value
1168 and control the generator torque in order to achieve the optimal tip-
1169 speed ratio (switch to Region 2).

1170 At low wind speeds, i.e. in partial load operation, variable-speed
1171 control is implemented to track the optimum point on the C_Q -surface
1172 for maximising the power output, which corresponds to the λ_{opt}
1173 value. The speed of the generator is controlled by regulating the de-
1174 manded torque $T_{g,d}$ on the generator through the generator torque
1175 controller. In partial load operation it is chosen to operate the wind
1176 turbine at $\beta = 0^\circ$, since the maximum power coefficient is obtained

at this pitch angle:

$$T_{g,d} = \frac{1}{2} \rho \pi R^2 \frac{R^3}{n_g^3 \lambda_{opt}^3} C_{max} \omega_g^2(t) - d_s \left(\frac{1}{n_g^2} + 1 \right) \omega_g(t) \quad (22)$$

1177 with n_g is the gear-ratio of the gearbox connecting the rotor shaft
1178 with the electric generator/converter, R is the rotor radius, and $\omega_g(t)$
1179 the electric generator/converter speed Johnson, Pao, Balas, and Fin-
1180 gersh (2006). The advantage of this approach is that only the mea-
1181 surement of the rotor or generator speed is required.
1182

1183 On the other hand, for high wind speeds, i.e. in full load operation,
1184 the desired operation of the wind turbine is to keep the rotor speed
1185 and the generated power at constant values. The main idea is to use
1186 the pitch system to control the efficiency of the aerodynamics, while
1187 applying the rated generator torque. However, in order to improve
1188 tracking of the power reference and cancel steady-state errors on the
1189 output power, a power controller is also introduced.

1190 With reference to the speed controller, it is implemented as a PI
1191 controller that is able to track the speed reference and cancel possi-
1192 ble steady-state errors on the generator speed. The speed controller
1193 transfer function $D_s(s)$ has the form:

$$D_s(s) = K_{ps} \left(1 + \frac{1}{T_{is}} \frac{1}{s} \right) \quad (23)$$

1194 where K_{ps} is the PI proportional gain and T_{is} is the reset rate of the
1195 integrator.

1196 The power controller is implemented in order to cancel possible
1197 steady-state errors in the output power. This suggests using slow in-
1198 tegral control for the power controller, as this will eventually cancel
1199 steady-state errors on the output power without interfering with the
1200 speed controller. However, it may be beneficial to make the power
1201 controller faster to improve accuracy in the tracking of the rated
1202 power. The power controller is realized as a PI controller, whose
1203 transfer function $D_p(s)$ has the standard form:

$$D_p(s) = K_{pp} \left(1 + \frac{1}{T_{ip}} \frac{1}{s} \right) \quad (24)$$

1204 where K_{pp} is the proportional gain of the PI regulator, whilst T_{ip} is the
1205 reset rate of the integrator.

1206 Note finally that speed and power control can be coupled. How-
1207 ever, as shown in Odgaard et al. (2013), they can be considered as
1208 decoupled, as their dynamics are different. However, more advanced
1209 control techniques can exploit multivariable (or decoupling) control,
1210 as addressed in Bianchi et al. (2007), Pao and Johnson (2011). It is
1211 worth noting that, from the previous considerations, the research is-
1212 sues of wind turbine control may seem very mature. However, the
1213 latest generation of giant offshore wind turbines present new dynam-
1214 ics and control issues.. Moreover, new wind turbine solutions, which

use further wind turbine state information from the sensing system, have been suggested, also within EU projects, see e.g. Plumley, Leithead, Jamieson, Bossanyi, and Graham (2014), Chatzopoulos and Leithead (2010). This improved state information is used to control the wind turbine blades and at the same time reducing the design bearing fatigue and extreme structural loads that are affecting the structure of the wind turbine Valencia-Palomo, Rossiter, and Lopez-Estrada (2014), Khan, Valencia-Palomo, Rossiter, Jones, and Gondhalekar (0000). This control problem will be solved in a multivariable way, by optimising the conflicting control objectives of power optimisation while keeping the different loads below the design requirements. The control goal is to ensure that the controller will guarantee that extreme load requirements are not violated during eventually emergency stops of the wind turbine, as well as during severe wind gusts. The interesting challenge is to be able to use the rotor system to control the turbine, so that in effect the rotor performs like a 'high level' sensor. In other words the goal is to be able to use the rotor itself (along with the enhanced sensor set) to make the control system perform well. A part of this challenge is to ensure that real-time compensation of loading and gust disturbances is put into effect in a suitable time window, taking account of the close spectral content of the disturbance and control. This becomes a very significant challenge for very large rotor wind turbines (> 10 MW) as the required control and disturbance bandwidths become close, a problem similar to the structural filtering and control used in high performance combat aircraft Shi and Patton (2015).

4.3. Control strategies for wave energy devices

As demonstrated in Fig. 5 the control problem first requires an optimum velocity profile to be calculated and this is then followed by controlling the PTO force. As documented in Section 3.4, there is significant focus on the hydrodynamic modelling aspects and this is also reflected in the balance of control studies devoted to the higher-level and lower-level depicted in Fig. 5. As a result, the focus here is mainly on hydrodynamic control (in Section 4.3.1), though some comments about lower level PTO control are given in Section 4.3.2.

4.3.1. Velocity profile calculation

Ignoring system constraints for the moment, a start can be made on the energy maximisation problem by considering the force-to-velocity model of a WEC, which is obtained from (21) in the frequency domain Falnes (2002) as:

$$\frac{V(\omega)}{F_{ex}(\omega) + F_u(\omega)} = \frac{1}{Z_i(\omega)} \quad (25)$$

where $Z_i(\omega)$ is termed the *intrinsic impedance* of the system. In (25), $V(\omega)$, $F_{ex}(\omega)$, and $F_u(\omega)$ represent the Fourier transform of the velocity $v(t)$, excitation force $f_{ex}(t)$, and control force $f_{PTO}(t)$, respectively. Unless stated otherwise, the Fourier transform of time-domain signals or functions will be denoted by the corresponding capital letter, namely $X(\omega) \triangleq \mathcal{F}\{x(t)\}$.

The intrinsic impedance $Z_i(\omega)$ of the model in (25) is specified as (see Falnes (2002) for the full derivation):

$$Z_i(\omega) = B_r(\omega) + j\omega \left[M + M_a(\omega) - \frac{K_b}{\omega^2} \right] \quad (26)$$

where $B_r(\omega)$ is the radiation resistance (real and even) and $M_a(\omega)$ is the frequency-dependent added mass, often replaced by its high-frequency asymptote m_∞ .

The model in (25) allows the derivation of conditions for optimal energy absorption and the intuitive design of the energy-maximising controller in the frequency-domain: Falnes (2002) as:

$$Z_{PTO}(\omega) = Z_i^*(\omega), \quad (27)$$

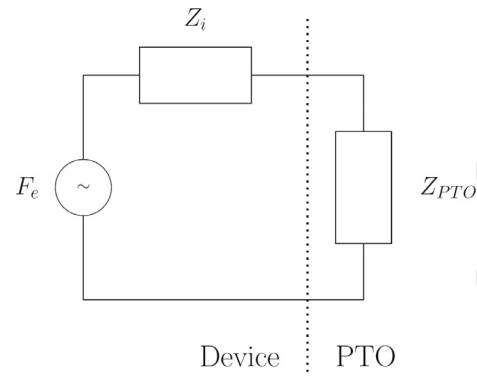


Fig. 14. Impedance matching problem for wave energy device.

where $(\cdot)^*$ denotes the complex conjugate. The choice of Z_{PTO} as in (27) is referred to as *complex conjugate control*, but many (especially electrical) engineers will recognise this choice of Z_{PTO} as the solution to the impedance-matching problem represented by Fig. 14. In Fig. 14, F_e represents the wave excitation force, while Z_i defines the relationship between this force and the device velocity, as determined by the WEC dynamics (see (26)). Under condition (27), maximum power is transferred from the device to the load, defined by Z_{PTO} , which is a well-known result for AC circuits.

The result in (27) has a number of important implications:

- The result is frequency dependent, implying that there is a different optimal impedance for each frequency, which raises the question of how to specify for irregular seas containing a mixture of frequencies;
- Since $h_r(t)$ is causal, $h_c(t) = \mathcal{F}^{-1}(Z_{PTO}(\omega))$ is anticausal, requiring future knowledge of the excitation force. While this knowledge is straightforward for the monochromatic case (single sinusoid), it is more problematic for irregular seas. However, some solutions are available, including those documented in Fusco and Ringwood (2010);
- Since force and velocity can have opposite signs in Fig. 14, the PTO may need to *supply* power for some parts of the sinusoidal cycle, which is akin to reactive power in electrical power systems. Such a phenomenon places particular demands on PTO systems, not only in terms of the need to facilitate bidirectional power flow, but also that the peak reactive power can be significantly greater than active power Shek, Macpherson, and Mueller (2008), Zurkinden, Guerinel, Alves, and Damkilde (2013). The optimal *passive* PTO is provided by $R_{PTO} = |Z_i(\omega)|$, which avoids the need for the PTO to supply power, but results in a suboptimal control;
- The optimal control in (27) takes no account of physical constraints in the WEC/PTO, where there are likely to be limitations on displacement or relative displacement, and the PTO force, and there may be external constraints imposed by electrical grid regulations;
- The maximum theoretical power recovered in an oscillating wave energy device is 50%, which represents the optimal matched condition in Fig. 14. Under such a condition, equal power is dissipated in the PTO and wave radiation, noting that a good wave energy absorber is also a good radiator Falnes (2002).

The condition in (27) can alternatively be expressed in terms of an optimal velocity profile as:

$$V^{opt}(\omega) = F_{ex}(\omega) / (2 R_i(\omega)), \quad (28)$$

where $R_i = 1/2 (Z_i + Z_i^*)$ is the real part of Z_i . The condition in (28) is a condition on the amplitude of $V^{opt}(\omega)$, with the restriction that $V^{opt}(t)$ be in phase with $f_{ex}(t)$, since R_i is a real (and even) function. This phase condition, considered separately, forms the basis for some

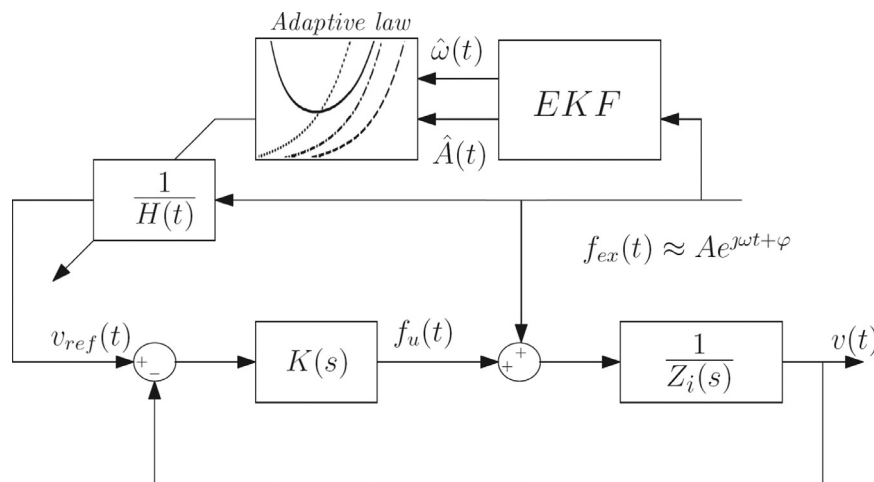


Fig. 15. Proposed control architecture for the simple controller. The EKF effectively tracks the wave frequency and amplitude as in (29), while the $1/H(t)$ block provides an adaptive feedforward gain to determine the optimal velocity profile.

1315 simple WEC phase control strategies, such as *latching* Budal and Falnes
1316 (1975), Babarit, Duclos, and Clement (2004).

1317 While the *complex conjugate control* resulting from the impedance
1318 matching problem provides the conceptual framework for optimal
1319 WEC control calculations, its implementation is not straightforward,
1320 for the reasons mentioned above. As a result, many alternatives
1321 have been proposed, many based on complex conjugate control,
1322 with the aim of being more suitable for implementation or real-time
1323 calculation.

1324 A simple development of the basic condition in (27) is suggested
1325 in Fusco and Ringwood (2013), which carries the assumption that
1326 $f_{ex}(t)$ is a narrow-banded harmonic process, defined by time-varying
1327 amplitude $A(t)$, frequency $\omega(t)$, and phase $\varphi(t)$ as:

$$f_{ex}(t) = A(t) \cos(\omega(t)t + \varphi(t)) \quad (29)$$

1328 The optimal reference velocity can then be generated from the adap-
1329 tive law

$$v_{ref}(t) = \frac{1}{H(t)} f_{ex}(t), \quad \frac{1}{H(t)} = \frac{1}{2R_i(\hat{\omega})} \quad (30)$$

1330 where the value of the constant $H(t)$ is calculated from the curve
1331 $1/2B(\omega)$, based on a real-time instantaneous estimate of the peak
1332 frequency of the wave excitation force. An on-line estimate of the
1333 frequency $\hat{\omega}$ and amplitude \hat{A} is obtained with the extended Kalman
1334 filter (EKF) Quine, Uhlmann, and Durrant-Whyte (1995). Based on the
1335 narrow-banded assumption of (29), the excitation force can be ex-
1336 pressed in complex notation as:

$$f_{ex}(t) = \Re \{ A e^{j\varphi} e^{j\omega t} \}, \quad \hat{F}_{ex} \triangleq A e^{j\varphi} \quad (31)$$

1337 where \hat{F}_{ex} is the complex amplitude of $f_{ex}(t)$, denoting $f_{ex}(t)$ as a single
1338 sinusoid with amplitude A and phase φ .

1339 As a consequence of the proportional reference-generation law in
1340 (30), the complex amplitude of the velocity \hat{V} and position \hat{U} can be
1341 expressed as:

$$\hat{V} = \frac{A}{H} e^{j\varphi} \quad (32)$$

$$\hat{U} = \frac{\hat{V}}{j\omega} = \frac{A}{j\omega H} e^{j\varphi} \quad (33)$$

1343 Suppose that the vertical excursion of the WEC is limited to $\pm U_{lim}$
1344 from equilibrium. From (33), the position constraint can be written
1345 as an equivalent velocity constraint:

$$\hat{U} = \frac{\hat{V}}{j\omega} \leq U_{lim} \Leftrightarrow |\hat{V}| \leq \omega U_{lim} \quad (34)$$

and an upper bound for the variable gain, $1/H$, involving the ampli-
1346 tude and frequency of the excitation, can be derived from (32) as:

$$\frac{1}{H} \leq \frac{\omega U_{lim}}{A} \quad (35)$$

1348 The reference generation strategy, based on (28), (30), and (35) can
1349 therefore be modulated to keep the amplitude of the velocity within
1350 the bound specified in (34). A real-time estimate of the frequency $\hat{\omega}$
1351 and amplitude \hat{A} of the excitation, can be obtained through the EKF
1352 Budal and Falnes (1982), Fusco and Ringwood (2010) and the feed-
1353 forward gain $\frac{1}{H(t)}$ adjusted according to:

$$\frac{1}{H(t)} = \begin{cases} \frac{1}{2R_i(\hat{\omega})}, & \text{if } \frac{\hat{\omega} U_{lim}}{\hat{A}} > \frac{1}{2R_i(\hat{\omega})} \\ \frac{\omega U_{lim}}{\hat{A}}, & \text{otherwise} \end{cases} \quad (36)$$

1354 According to (36), when in the unconstrained region, the velocity is
1355 tuned to the optimal amplitude given by complex-conjugate control,
1356 as in (28). Otherwise, the maximum allowed velocity (lower than the
1357 optimal) is imposed, while keeping the velocity in phase with the ex-
1358 citation force. The control structure is illustrated in Fig. 15.

1359 Other control architectures have also been proposed, including,
1360 for example, those based on numerical optimisation. Though the per-
1361 formance function to be maximised is somewhat non-traditional,
1362 namely:

$$J(T, f_{pto}) = \int_0^T f_{pto}(t) v(t) dt \quad (37)$$

1363 where f_{pto} is the PTO force and $v(t)$ the velocity profile of the device,
1364 a number of control methods having their origins in mainstream con-
1365 trol have been customised for use in a wave energy context. These in-
1366 clude model predictive control Hals, Falnes, and Moan (2011), Cretel,
1367 Lightbody, Thomas, and Lewis (2011), Brekken (2011), Richter, Ma-
1368 gaña, Sawodny, and Brekken (2013a), Li and Belmont (2014) and a
1369 numerical optimisation method using a pseudo-spectral parameteri-
1370 sation Garcia-Rosa et al. (2015a). A reasonably comprehensive review
1371 of control strategies for WECs is given in Ringwood et al. (2014).

1372 One of the significant challenges in wave energy control is that of
1373 the assumption of model linearity. Many hydrodynamic models are
1374 linearised around the SWL. This follows a relative normal practice in
1375 traditional control, but is somewhat less valid in the case of wave en-
1376 ergy, where the general objective is to exaggerate the device motion,
1377 rather than drive the system to an equilibrium point. More recently,
1378 control algorithms for WECs have begun to emerge which deal with
1379 various nonlinear aspects, including:

- 1380 • Nonlinear hydrodynamic restoring force [Richter, na, Sawodny, and](#)
1381 [Brekken \(2013b\)](#);
- 1382 • Viscous drag resulting from relatively high body/fluid motions
1383 [Bacelli and Ringwood \(2014\)](#);
- 1384 • Non-ideal PTO effects [ao and Henriques \(2015\)](#), [Genest, Bonnefoy,](#)
1385 [Clément, and Babarit \(2014\)](#), [Becelli, Genest, and Ringwood \(in](#)
1386 [press\)](#).

1387 However, controllers dealing with fully nonlinear hydrodynamics
1388 (for example, incorporating nonlinear dynamic Froude–Krylov forces)
1389 have yet to be developed.

1390 4.3.2. PTO force control

1391 Given the range of PTO control inputs as shown in [Fig. 11](#) and the
1392 wide variety of PTO systems employed on prototype WECs, there is
1393 little convergence on PTO control system design. However, PTO con-
1394 trol represents a traditional tracking control problem, to which a wide
1395 variety of conventional control strategies can be employed.

1396 A number of studies have documented lower-loop control strate-
1397 gies for WEC PTO systems, including solutions based on Internal
1398 Model Control (IMC) [Fusco and Ringwood \(2013\)](#), [ao, Mendes, Valério,](#)
1399 [and Costa \(2007\)](#) and Proportional–Integral–Plus (PIP) control [Taylor,](#)
1400 [Stables, Cross, Gunn, and Aggidis \(2009\)](#). A robust control strategy, using
1401 a passivity-based controller, is presented in [Fusco and Ringwood](#).
1402 In some cases an integrated high/low-level controller is employed as,
1403 for example in [Falcão \(2007\)](#), for a two-body WEC with a hydraulic
1404 PTO system.

1405 4.4. Comparisons and contrasts of wind and wave control systems

1406 Given the more mature development of wind turbines, consider-
1407 ably more attention has been focussed on the wind turbine control
1408 problem, resulting in refined control systems which can undertake a
1409 variety of functions, including:

- 1410 • Optimal set–point generation;
- 1411 • Turbine speed and torque control (setpoint following);
- 1412 • Supervisory control of the turbine, considering the different oper-
1413 ation requirements under the various scenarios in [Fig. 2](#).

1414 In addition, various advanced strategies, such as fault tolerant con-
1415 trol, have also been developed for wind turbines, as articulated in
1416 [Section 5.1](#).

1417 It is clear that various ‘levels’ of control are required in both ocean
1418 energy and wind turbine applications. There is a top level of super-
1419 visory control which assesses the incident energy resource and may
1420 curtail the operation of the device in the face of extreme conditions.
1421 Such curtailment may be requirement in order to preserve the device
1422 integrity, ensure safe operation, or be required by legislation, as in
1423 the case of wind turbines. This is the case when wind turbines work
1424 in full load conditions, *i.e.* above the rated wind speed. On the other
1425 hand, they are designed to operate in the energy capture mode, *i.e.*
1426 below the rated wind speed. This working condition is similar to the
1427 WECs, where maximum–energy transfer is required. However, wave
1428 energy devices will frequently encounter sea states which are out-
1429 side their normal operational envelope and some supervisory strate-
1430 gy may be necessary to ensure that device integrity is retained.
1431 Such supervisory control is important, and it can represent an im-
1432 portant issue also for the safety of wind turbines, as briefly outlined
1433 in [Section 5.1](#).

1434 Finally, one control aspect which is contrasting between wind and
1435 wave applications is the relative benefit of controlling an array of de-
1436 vices in a co-ordinated way. For wind farms, only destructive inter-
1437 ference occurs between neighbouring turbines due to wind shadow
1438 effects. For wave energy device farms, however, both constructive and
1439 destructive interference may occur. The optimal operation of both
1440 wind and wave farms is a significant function of the farm layout,

1441 which depends on the land topography and the wind direction prob-
1442 ability distribution. However, in the wave energy case, for a given
1443 device layout, co-ordinated control of device motions may optimise
1444 constructive device interference (since each moving device radiates
1445 waves), resulting in potential gains of up to 20% in captured energy
1446 [Bacelli et al. \(2013a\)](#), [Bacelli and Ringwood \(2013a\)](#). It has also been
1447 shown that, for the wave energy case, that there is significant inter-
1448 action between the control system employed and the optimal WEC
1449 array layout, from an energy capture perspective [Garcia-Rosa et al.](#)
1450 [\(2015a\)](#).

1451 It is worth noting that, with reference to wind farms, the turbines
1452 are usually positioned to minimise down–wind interaction, so the
1453 interaction effects are minimal. This means that the distributed and
1454 de–centralised control of farms is mainly a subject of electrical load
1455 balancing rather than distributed aspects of aero–mechanical rotor
1456 control. However, some recent studies have been performed in or-
1457 der to decouple the interaction effects among the wind turbines of
1458 a wind farm [Simani, Farsoni, Castaldi, and Mimmo \(2015b\)](#), [Simani,](#)
1459 [Farsoni, and Castaldi \(2015a\)](#). The situation with arrays of wave en-
1460 ergy converters is different, where the interaction between relatively
1461 close WECs (point absorbers, *etc*) in an array can be considered to be
1462 significant. Oscillating WECs generate radiation waves covering a sig-
1463 nificant area, with resulting possibilities for both positive and nega-
1464 tive reinforcement of the incident wave excitation, for any particular
1465 device.

1466 To this end, wave energy arrays need to be carefully laid out, but
1467 centralised (global) array control algorithms can play a significant
1468 part in maximising the benefit of mutual radiation effects [Bacelli,](#)
1469 [P. Balitsky, and Ringwood \(2013b\)](#), [Bacelli and Ringwood \(2013d\)](#),
1470 where a complete model of the hydrodynamic interactions is avail-
1471 able. It has also been shown that there is significant interaction be-
1472 tween the optimal WEC array layout problem and the global WEC
1473 array control problem *i.e.* the optimal WEC array layout depends on
1474 the WEC array control strategy employed [Garcia-Rosa, Costello, Dias,](#)
1475 [and Ringwood \(2015b\)](#).

1476 5. Towards the future

1477 The variability of the power produced from renewable sources and
1478 its uncontrollable nature negatively affects their effectiveness in re-
1479 ducing the requirement for thermal plants (it reduces their capacity
1480 credit) and makes them a less attractive and a potentially more ex-
1481 pensive alternative. Wind and wave energy, however, offer important
1482 and significant energy resources and can be of major assistance in
1483 mitigating climate change, so it is imperative that maximum effort
1484 be devoted to refining the technology (including control technology)
1485 used to convert these resources to a useful and economic form.

1486 This paper focusses on the analysis and the comparison between
1487 the two resources, considering also the variability of the power ex-
1488 traction when wind or wave offshore farms are adopted, with respect
1489 to the exploitation of the renewable resources. It can be noted that, in
1490 some cases, wave systems where the predominant (from an energy
1491 point of view) part is composed of large swell systems, generated
1492 by remote wind systems, have little correlation with the local wind
1493 conditions. This means that the two resources can appear at different
1494 times and, if considered together, their integration in combined
1495 farms allows a more reliable, less variable and more predictable
1496 electrical power production [Babarit et al. \(2006\)](#), [Fusco et al. \(2010\)](#).
1497 The reliability is improved thanks to a significant reduction of the pe-
1498 riods of null or very low power production (which is a problem with
1499 wind farms). The variability and predictability improvements derive
1500 from the smoothing effect due to the integration of poorly correlated
1501 diversified sources. To this end, a number of combined offshore
1502 wind/wave platforms have also been proposed [Soulard, Babarit,](#)
1503 [Borgarino, Wyns, and Harismendy \(2013\)](#). Combined wind/wave
1504 installations also have the significant benefit of sharing electrical and

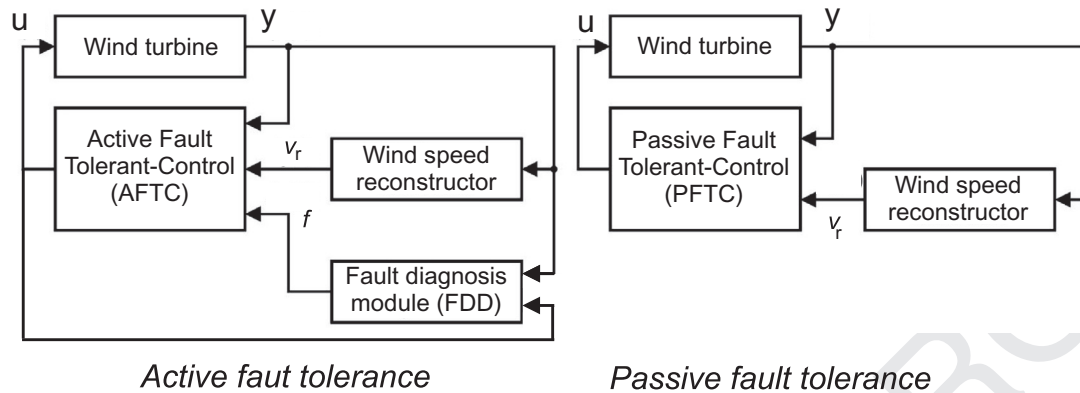


Fig. 16. Structure of the active and passive fault-tolerant control systems.

civil engineering infrastructure. This may help to reduce overall costs, though it is also likely that there is some compromise in the level of optimality of the individual wind or wave resources, in such cases.

On the other hand, in some other cases, the combination of wind and waves does not appear to be an attractive solution, due to a limited wave energy resource, which is strongly correlated to the local wind conditions Fusco et al. (2010). The conclusion is, then, that the potential benefits of the integration of wind and wave resources, where the climate of the location is appropriate, are too important to be neglected. This paper attempts to highlight the quantification of these benefits, particularly from a raw resource assessment point of view. With wave energy technology becoming more mature, it should be possible to develop a more complete analysis where these benefits are integrated, together with the actual costs of the different wave and wind technologies, in a global functional, whose optimisation should lead to a proper dimensioning and design of offshore combined farms, given the energy climate of a particular location.

Note finally that, as the world's power supply depends to an every greater extent on renewable resources, it is consequently and increasingly important that these are as reliable and predictable as possible, so that effective economic dispatch can be performed. So-called Fault Tolerant Control (FTC) Blanke et al. (2006) can play a substantial part in increasing reliability of modern wind turbines and wave energy devices. This is especially true for remote marine locations, where access and weather windows make regular and immediate maintenance problematic, and FTC can significantly increase energy conversion productivity by providing some level of energy supply during certain fault conditions.

Benchmark models for wind turbine and wind farm fault detection and isolation, and FTC have previously been proposed Odgaard and Stoustrup (2013), Odgaard and Stoustrup (0000). Based on this benchmarks, an international competitions on wind turbine fault diagnosis and FTC were announced Odgaard and Odgaard (2012), Odgaard and Shafiei (0000). Under these considerations, Section 5.1 summarises advanced methods that show potential for wind turbine fault diagnosis and FTC. In addition, as they highlighted good performance, these approaches are also relevant for industrial usage. This means that the wind turbine controller can continue operation as in the fault-free case.

In contrast, however, there have been few studies which compare either different modelling or different control strategies for WECs. This is a significant limitation in making an assessment of true progress in the state-of-the-art. While there are a wide variety of WEC concepts, and different WECs may benefit from different customised modelling and control solutions, some benchmark comparisons are necessary. Some progress, in this regard, is being made with the recent COER hydrodynamic modelling competition Garcia-Rosa et al. (2015b), which provided a benchmark data set from tank testing

of a WEC-like device, while a WEC control benchmark competition is currently in the early stages of organisation.

However, while FTC (and associated benchmark problems) are becoming popular in wind turbine control research, wave energy systems lag far behind, in spite of perhaps a greater imperative for fault-tolerant systems, due to more severe access limitations. However, the benchmark problems and FTC solutions developed in the wind energy research community can provide a useful model that the wave community can learn from.

5.1. Advanced methods in wind turbine control

Over the last decade, many studies have been carried out on wind turbine fault diagnosis, with the most relevant including Gong and Qiao (2013), Estima, and Cardoso (2013). In addition, the FTC problem for wind turbines was recently analysed with reference to an offshore wind turbine benchmark e.g. in Odgaard et al. (2013). In general, FTC methods are classified into two types, i.e. Passive Fault Tolerant Control (PFTC) scheme and Active Fault Tolerant Control (AFTC) scheme Mahmoud et al. (2003). In PFTC, controllers are fixed and are designed to be robust against a class of presumed faults. In contrast to PFTC, AFTC reacts to the system component failures actively by reconfiguring control actions so that the stability and acceptable performance of the entire system can be maintained. Therefore, the term 'sustainable' is used to characterise wind turbine control, and it represents a challenging task.

In order to outline and compare the controllers developed using active and passive fault-tolerant design approaches, they should be derived using the same procedures in the fault-free case. In this way, any differences in their performance or design complexity would be caused only by the fault tolerance approach, rather than the underlying control solutions Bianchi et al. (2007), Galdi, Piccolo, and Siano (0000).

The two FTC solutions have different structures as shown in Fig. 16. Note that only AFTC relies on a fault diagnosis algorithm (FDD). This represents the main difference between the two control schemes.

The main connection between AFTC and PFTC schemes is that an AFTC relies on a fault diagnosis system, which provides information about the faults f to the controller. In the considered case, the Fault Detection and Diagnosis (FDD) system contains the estimation of the unknown input (fault) affecting the system under control. The knowledge of the fault f allows the AFTC to reconfigure the current state of the system. On the other hand, the FDD is able to improve the controller performance in fault-free conditions, since it can compensate modelling errors, uncertainty and disturbances. On the other hand, the PFTC scheme does not rely on a fault diagnosis algorithm, but is designed to be robust towards any possible faults.

This is accomplished by designing a controller that is optimised for the fault-free situation, while satisfying some graceful degradation requirements in the faulty cases. However, with respect to the robust control design, the PFTC strategy provides reliable controllers that guarantee the same performance with no risk of false fault detection or reconfigurations.

Clearly, the issues addressed by such FTC schemes for wind turbines are no less relevant for wave energy applications. In fact, the issue is likely to be even more manifest where wave energy devices are located far offshore (the location of the greatest wave energy) and access for maintenance and repair may be difficult [Odgaard \(2012\)](#). Such an issue is, of course, also relevant for those wind turbines located offshore though, in such cases, preference is usually given to sites which present relatively shallow water depth. However, recent developments in floating wind and wave platforms [Soulard et al. \(2013\)](#) may present composite challenges, but they are not considered in this paper.

5.2. Overall economic considerations

While control systems are ostensibly added in order to maximise power capture, care must be taken that such control systems have no adverse effect on the system. Though raw wind and wave energy are essentially free, the systems to convert this raw energy are not and, ultimately, the receipts from energy sales are balanced to some extent by significant capital and operational costs. In the offshore environment, it is estimated that capital and operational costs are in roughly equal proportion.

One important aspect in this economic perspective is to consider if the addition of a control system may drive the system more aggressively in an attempt to increase energy capture, perhaps leading to shortened device lifetimes. While the addition of control to a wind turbine is likely to be relatively benign, the use of motion-exaggerating control for a reciprocating wave energy device can have a dramatic effect on device motion. Consequently, the balance between increased energy capture (income) and increased device wear (cost) needs to be carefully considered. It is also known, for example, that the use of reactive control, where some energy from the grid side is used to exaggerate device motion (capturing more net energy overall) in WEC control brings significantly increased requirements in system power capacity [Shek, Macpherson, Mueller, and Xiang \(2007\)](#).

While potentially effecting more aggressive device motion, there are some redeeming features of control which may help the designer in practical applications. For example, physical constraints can be explicitly included in many control formulations, resulting in a control action that respects (and is optimal within) the physical system constraints. In addition, for both wind turbines and WECs, most optimal control formulations allow some explicit trade-off between control action and the main objective (e.g. setpoint tracking, energy maximisation, etc), which provides a design handle on the level of aggressiveness of the control. Control science also provides a body of knowledge relating to the design of control systems which are tolerant (in some respect, but usually with reduced performance) to system, actuator or sensor faults or malfunctions, as described in [Section 5.1](#).

It has also been shown that there is often significant interaction between the optimal (uncontrolled) device design and the control system used to optimise its behaviour. For example in the wave energy context, where controllers are effectively used to extend the bandwidth of WECs so they can operate effectively across a wide variety of sea conditions, the uncontrolled (open loop) device resonant frequency should be carefully placed, so that the controller can take maximum advantage [Garcia-Rosa and Ringwood](#). For example, latching control [Babarit and Clement \(2006\)](#) can extend the WEC frequency response in the direction of lower frequencies, suggesting that the (uncontrolled) resonant frequency of the WEC should be small. This has a double benefit in ensuring an optimal

WEC/controller combination, while also requiring a smaller device, with potentially lower capital costs.

In the wind turbine case, significant advances in turbine control have led to a situation where turbine developers are providing progressively less control power, so that control energy consumption is minimised. However, this reaction, in turn, leads to highly nonlinear control action, since the control signals are regularly saturating, increasing the control challenge still further [Leithead and Connor \(2000\)](#).

6. Conclusion

The motivation for this paper came from the need to have an overview about the main challenges of modelling and control for wind turbines and wave energy devices. In order to present common and different requirements over power conversion efficiency (i.e. the renewable source power that can be converted into electric energy, the work focussed on commonalities and contrasts for these two fields.

Therefore, the analysis of the commonalities and the contrasts between these two fields was mainly performed according the items below:

- System model purpose;
- Renewable resource descriptions;
- Control strategy development.

On the basis of these items, the following considerations have been finally outlined. On one hand, wind turbine systems seem relatively mature from the modelling point of view, whilst wave energy devices still present challenging modelling issues. This remark is valid for medium size wind turbines: large rotor installations can drive challenging and complex modelling and control issues.

Both wind turbine and wave energy control systems can share a common structure. In addition to these components, a further level of supervisory control is required to correctly select the control strategy appropriate to the model of operation, usually dictated by the prevalent wind or wave resource measure. For the wind turbine case, such operational modes are well defined, as articulated in terms of the various sections of the power curve. However, though the overall number of operational modes may be lower, wave devices also have a cut-in power level below which energy conversion is not economic/possible, a main power production region where energy conversion should be maximised, a region where energy conversion must be curtailed due to the capacity of (for example) electrical components and, finally, a survival mode where energy production is abandoned and system motion configured to avoid potential structural damage. The means by which survivability is managed in the wave case is not as straightforward as in wind, due to the wide variety of wave devices and the difficulty of finding an orientation or configuration which avoids the destructive influence of high wave energy fluxes.

Despite the differences in relative maturity of wind and wave energy, both share many fundamental principles, including the fact that only a fraction of the raw wind (60%) and wave (50%) resources can be usefully converted, at best. These limitations relate to basic aerodynamic (wind) and hydrodynamic (wave) considerations.

In general, both wave and wind energy conversion systems require a high degree of availability, as it significantly affects the final energy cost. Moreover, these systems have highly nonlinear dynamics, with stochastic inputs, in the form of wind and wave driving forces. Suitable control methods should provide the optimisation of the energy conversion efficiency over wider than normally expected working conditions. Moreover, it was shown that proper mathematical descriptions were necessary to capture the complete behaviour of the systems under consideration, thus providing an important impact on the control design itself.

On the basis of these considerations, it seems that the considered two domains can be only partially compared. The modelling of these systems is quite different, but the control principle (if limited to the wind turbine partial load condition) is similar. Also the intermittent resources that drive them are, in many cases, uncorrelated, leading to the advantageous combination of both technologies. However, the technological challenge, from a modelling and control perspective, coupled with the high cost of offshore deployment and maintenance, helps to explain why wind turbines are now commonplace, whilst wave energy devices are not.

Acknowledgements

J.V. Ringwood is grateful to the Irish Marine Institute for the data pertaining to Fig. 9 and to Pelamis Wave Power for Fig. 4. The research of J.V. Ringwood is supported by Science Foundation Ireland under grant no. 12/RC/2302 for the Marine Renewable Ireland (MaREI) centre and by Investigator Award 13/IA/1886. S. Simani wishes to acknowledge Prof. Ron J. Patton of The University of Hull (Hull, UK) for his helpful discussions. Finally, S. Simani is also grateful to Dr. Peter Fogh Odgaard of Aalborg University (Aalborg, Denmark) and Prof. Horst Schulte of the HTW University of Applied Sciences (Berlin, Germany) for the details on wind turbine simulators.

References

- Adegas, F., Sloth, C., & Stoustrup, J. (2012). Control of linear parameter varying systems with applications. *Structured linear parameter varying control of wind turbines* (1st, pp. 303–337). London: Springer–Verlag. doi:10.1007/978-1-4614-1833-7.
- Adegas, F. D., Sonderby, I. B., Hansen, M. H., & Stoustrup, J. (2013). Reduced-order LPV model of flexible wind turbines. *Proceedings of the 2013 IEEE Multi-conference on Systems and Control* (pp. 424–429). Hyderabad, India: IEEE. doi:10.1109/CCA.2013.6662786.
- Adegas, F. D., & Stoustrup, J. (2011). Robust structured control design via LMI optimization. In *Proceedings of the 18th IFAC world congress, IFAC, IFAC, milan, italy* (pp. 7933–7938).
- Adegas, F. D., & Stoustrup, J. (2012). Structured control of LPV systems with application to wind turbines. In *Proceedings of the 2012 American control conference, IEEE, IEEE, Montreal, Canada* (pp. 756–761). doi:10.1109/ACC.2012.6315456.
- Agamloh, E. B., Wallace, A. K., & von Jouanne, A. (2008). Application of fluid structure interaction simulation of an ocean wave energy extraction device. *Renewable Energy*, 33(4), 748–757.
- Falcão, A. F. d. O. (2007). Modelling and control of oscillating-body wave energy converters with hydraulic power take-off and gas accumulator. *Ocean Engineering*, 34(14–15), 2021–2032.
- ao, A. F. F., & Henriques, J. C. (2015). Effect of non-ideal power take-off efficiency on performance of single- and two-body reactively controlled wave energy converters. *Journal of Ocean Engineering and Marine Energy*, 1–14.
- ao, P. B., Mendes, M. J. G. C., Valério, D., & Costa, J. S. D. (2007). Control of the archimedes wave swing using neural networks. In *Proceedings of the European wave and tidal energy conference (EWTEC)*.
- Babarit, A., Ahmed, H. B., Clément, A., Debusschere, V., Duclos, G., Multon, B., et al. (2006). Simulation of electricity supply of an atlantic island by offshore wind turbines and wave energy converters associated with a medium scale local energy storage. *Renewable Energy*, 31(2), 153–160.
- Babarit, A., & Clement, A. (2006). Optimal latching control of a wave energy device in regular and irregular waves. *Applied Ocean Research*, 28, 77–91.
- Babarit, A., Duclos, G., & Clement, A. (2004). Comparison of latching control strategies for a heaving wave energy device in random sea. *Applied Ocean Research*, 26(5), 227–238.
- Bacelli, G., Balitsky, P., & Ringwood, J. (2013a). Coordinated control of arrays of wave energy devices - benefits over independent control. *IEEE Transaction on Sustainable Energy*, 4, 1091–1099.
- Bacelli, G., Gilloteaux, J.-C., & Ringwood, J. (2008). State space model of a hydraulic power take off unit for wave energy conversion employing bondgraphs. In *Proceedings of World renewable energy conference*.
- Bacelli, G., P. Balitsky, J., & Ringwood, V. (2013b). Coordinated control of arrays of wave energy devices benefits over independent control. *IEEE Transactions on Sustainable Energy*, 4(4), 1091–1099.
- Bacelli, G., & Ringwood, J. (2013a). Constrained control of arrays of wave energy devices. *International Journal of Marine Energy*, 3(4), e53–e69.
- Bacelli, G., & Ringwood, J. (2013b). Constrained control of arrays of wave energy devices. In *Proceedings 11th european wave energy conference, Aalborg, Denmark*.
- Bacelli, G., & Ringwood, J. (2013c). A geometric tool for the analysis of position and force constraints in wave energy converters. *Ocean Engineering*, 65, 10–18.
- Bacelli, G., & Ringwood, J. (2014). Nonlinear optimal wave energy converter control with application to a flap-type device. In *Proceedings of the 19th ifac World congress* (pp. 7696–7701).
- Bacelli, G., & Ringwood, J. V. (2013d). Constrained control of arrays of wave energy devices. *International Journal of Marine Energy*, 34, e53–e69.
- Becelli, G., Genest, R., Ringwood, J., Nonlinear control of flap-type wave energy converter with a non-ideal power take-off system, *IFAC Annual Control Reviews* in press.
- Betz, A., & Randall, D. G. (1966). *Introduction to the theory of flow machines*. Oxford: Pergamon Press. ISBN: 978-0080114330
- Bhinder, M., Babarit, A., Gentaz, L., & Ferrant, P. (2012). Effect of viscous forces on the performance of a surging wave energy converter. In *Proceedings of the international society of offshore and polar engineers (ISOPE)* (pp. 545–550).
- Bianchi, F. D., Battista, H. D., & Mantz, R. J. (2007). Wind turbine control systems: principles, modelling and gain scheduling design. *Advances in Industrial Control* (1st). Springer. ISBN: 1-84628-492-9
- Biegel, B., Madjidian, D., Spudic, V., Rantzer, A., & Stoustrup, J. (2013). Distributed low-complexity controller for wind power plant in derated operation. In *Proceedings of the 2013 IEEE multi-conference on systems and control, IEEE, IEEE, Hyderabad, India* (pp. 146–151). doi:10.1109/CCA.2013.6662758.
- Blanke, M., Kinnaert, M., Lunze, J., & Staroswiecki, M. (2006). *Diagnosis and Fault-Tolerant Control*. Berlin, Germany: Springer–Verlag.
- Bossanyi, E. A. (2003). Individual blade pitch control for load reduction. *Wind Energy*, 6(1), 119–128.
- Bossanyi, E. A., & Hassan, G. (2000). The design of closed loop controllers for wind turbines. *Wind Energy*, 3(3), 149–164. John Wiley & Sons, Ltd. doi:10.1002/we.34.
- Bottasso, C. L., Croce, A., & Savini, B. (2007). *Performance comparison of control schemes for variable-speed wind turbines: 75 p.* 012079. IOP Publishing. doi:10.1088/1742-6596/75/1/012079.
- Brekken, T. (2011). On model predictive control for a point absorber wave energy converter. In *Proceedings of IEEE powertech, Trondheim* (pp. 1–8).
- Bretschneider, C. (1952). The generation and decay of wind waves in deep water. *Transactions of the American Geophysical Union*, 33, 381–389.
- Budal, K., & Falnes, J. (1975). A resonant point absorber of ocean wave power. *Nature*, 256, 478–479.
- Budal, K., & Falnes, J. (1982). The Norwegian wave-power buoy project. In *Proceedings of the second international symposium on wave energy utilization* (pp. 323–344).
- Burton, T., Sharpe, D., Jenkins, N., & Bossanyi, E. (2011). *Wind Energy Handbook* (2nd). New York: John Wiley & Sons.
- Chatzopoulos, A.-P., & Leithead, W. E. (2010). Reducing tower fatigue loads by a co-ordinated control of the supergen 2MW exemplar wind turbine. In *Proceedings of the 3rd torque 2010 conference, Heraklion, Crete, Greece* (pp. 667–674).
- Chen, J., & Patton, R. J. (1999). *Robust model-based fault diagnosis for dynamic systems*. Boston, MA, USA: Kluwer Academic Publishers.
- Cleary, P., Prakash, M., Ha, J., Stokes, N., & Scott, C. (2007). Smooth particle hydrodynamics: status and future potential. *Progress in Computational Fluid Dynamics*, 7, 740–90.
- Clement, A. (2009). Using differential properties of the green function in seakeeping computational codes. In *Proceedings of the European control conference* (pp. 3755–3760).
- Costello, R., Teillant, B., & Ringwood, J. (2012). Techno-economic optimisation for wave energy converters. In *Proceedings of the 4th international conference on ocean energy (ICOE), Dublin, Ireland* (pp. 1–5).
- World Energy Council, (Ed.) (2013). *Cost of energy technologies, world energy perspective*. London, UK: World Energy Council. ISBN: 9780946121304. Available at: www.worldenergy.org.
- Cretel, J. A. M., Lightbody, G., Thomas, G. P., & Lewis, A. W. (2011). Maximisation of energy capture by a wave-energy point absorber using model predictive control. In *Proceedings of Ifac World congress*.
- Cummins, W. (1962). The impulse response function and ship motions. *Schiffstechnik*, 9, 101–109.
- Cutululis, N. A., Ceanga, E., Hansen, A. D., & Sorensen, P. (2006). Robust multi-model control of an autonomous wind power system. *Wind Energy*, 9(5), 399–419. doi:10.1002/we.194.
- Davidson, J., Giorgi, S., & Ringwood, J. (2013). Linear parametric hydrodynamic models based on numerical wave tank experiments. In *Proceedings of the 9th European wave and tidal energy conference (EWTEC), Aalborg*.
- De Andres, A., Guanche, R., Vidal, C., & Losada, I. (2015). Adaptability of a generic wave energy converter to different climate conditions. *Renewable Energy*, 78, 322–333.
- Diaz-Guerra, L., Adegas, F. D., & Stoustrup, J. (2012). Adaptive control algorithm for improving power capture of wind turbines in turbulent winds. In *Proceedings of the 2012 American control conference, IEEE, IEEE, Montreal, Canada* (pp. 5807–5812).
- Ding, S. X. (2008). *Model-based fault diagnosis techniques: design schemes, algorithms, and tools* (1st). Berlin Heidelberg: Springer. ISBN: 978-3540763031.
- Drew, B., Plummer, A., & Sahinaya, M. (2009). A review of wave energy converter technology. *Proceedings of the Institution of Mechanical Engineers Part A: Power and Energy*, 223, 887–902.
- Eriksson, M., Waters, R., Svensson, O., Isberg, J., & Leijon, M. (2007). Wave power absorption: Experiments in open sea and simulation. *Journal of Applied Physics*, 102(8), 084910–084910–5, DOI: <http://dx.doi.org/10.1063/1.2801002>.
- Falnes, J. (2002). *Ocean waves and oscillating systems*. Cambridge, UK: Cambridge University Press.
- Freire, N. M. A., Estima, J. O., & Cardoso, A. J. M. (2013). Open-circuit fault diagnosis in PMSG drives for wind turbine applications. *IEEE Transaction on Industrial Electronics*, 60(9), 3957–3967.
- Friis, J., Nielsen, E., Bonding, J., Adegas, F. D., Stoustrup, J., & Odgaard, P. F. (2011). Repetitive model predictive approach to individual pitch control of wind turbines. In *Proceedings of the IEEE CDC & ECC 2011, IEEE, IEEE, Orlando, FL, USA* (pp. 3664–3670).
- Froude, R. E. (1889). On the part played in propulsion by difference in pressure. *Transaction of the Institute of Naval Architects*, 30, 390–423.

- Fusco, F., Nolan, G., & Ringwood, J. V. (2010). Variability reduction through optimal combination of wind/wave resources—an Irish case study. *Energy*, 35(1), 314–325.
- Fusco, F., Ringwood, J., Hierarchical robust control of oscillating wave energy converters with uncertain dynamics. *IEEE Transaction on Sustainable Energy*.
- Fusco, F., & Ringwood, J. (2010). Short-term wave forecasting for real-time control of wave energy converters. *IEEE Transaction on Sustainable Energy*, 1(2), 99–106.
- Fusco, F., & Ringwood, J. (2013). A simple and effective real-time controller for wave energy converters. *IEEE Transaction on Sustainable Energy*, 4, 21–30.
- Galdi, V., Piccolo, A., Siano, P. Designing an adaptive fuzzy controller for maximum wind energy extraction. *IEEE Transactions on Energy Conversion* 23 (2).
- Garcia-Rosa, P., Bacelli, G., & Ringwood, J. (2015a). Control-informed optimal array layout for wave farms. *IEEE Transaction on Sustainable Energy*, 6(2), 575–582.
- Garcia-Rosa, P. B., Costello, R., Dias, F., & Ringwood, J. V. (2015b). Hydrodynamic modelling competition-overview and approaches. In *Proceedings of the international conference on offshore mechanics and arctic engineering*.
- Garcia-Rosa, P. B., Ringwood, J. V., On the sensitivity of optimal wave energy device geometry to the energy maximizing control system, *IEEE Transaction on Sustainable Energy* in press.
- Gasch, R., & Tvele, J. (2012). *Wind power plants: fundamentals, design, construction and operation* (2nd). Springer. ISBN: 978-3642229374.
- Genest, R., Bonnefoy, F., Clément, A. H., & Babarit, A. (2014). Effect of non-ideal power take-off on the energy absorption of a reactively controlled one degree of freedom wave energy converter. *Applied Ocean Research*, 48, 236–243.
- Gilloteaux, J.-C., & Ringwood, J. (2009). Influence of wave directionality on a generic point absorber. In *Proceedings of the 8th European wave and tidal energy conference, Uppsala, Sweden* (pp. 979–988).
- Gong, X., & Qiao, W. (2013). Bearing fault diagnosis for direct-drive wind turbines via current-demodulated signals. *IEEE Transactions on Industrial Electronics*, 60(8), 3419–3428. doi:10.1109/TIE.2013.2238871.
- Hals, J. (2010). *Modelling and phase control of wave energy converters*. Norwegian University of Science and Technology (Ph.D. thesis).
- Hals, J., Falnes, J., & Moan, T. (2011). Constrained optimal control of a heaving buoy wave-energy converter. *Journal of Offshore Mechanics and Arctic Engineering*, 133(1), 011401.
- Hansen, M. (2011). Aeroelastic properties of backward swept blades. In *Proceedings of the 49th AIAA aerospace sciences, AIAA, Orlando, Florida, USA* (pp. 1–19).
- Hasselmann, K. (1973). Measurements of wind-wave growth and swell decay during the joint north sea wave project (JONSWAP). *Tech. rep. Deutschen Hydrographischen Institut, Hamburg, Germany*.
- Heier, S. (2014). Grid integration of wind energy: onshore and offshore conversion systems. In *Engineering & Transportation* (3rd ed.). John Wiley & Sons Ltd. ISBN: 978-1119962946.
- International, E. (2005). Accessible wave energy resource atlas: Ireland: 2005. In *The marine institute/sustainable energy Ireland*.
- Ioannou, P., & Sun, J. (1996). *Robust adaptive control*. Upper Saddle River, NJ, USA: PTR Prentice-Hall.
- Johnson, K. E., Pao, L. Y., Balas, M. J., & Fingersh, L. J. (2006). Control of variable-speed wind turbines: standard and adaptive techniques for maximizing energy capture. *IEEE Control Systems Magazine*, 26(3), 70–81. doi:10.1109/MCS.2006.1636311.
- Jonkman, J., Butterfield, S., Musial, W., & Scott, G. (2009). Definition of a 5-MW reference wind turbine for offshore system development. *Tech. rep. NREL/TP-500-38060*. National Renewable Energy Laboratory, Golden, CO, USA.
- Jonkman, J. M., & Buhl Jr, M. L. (2005). FAST user's guide. *Tech. rep. NREL/EL-500-38230*. National Renewable Energy Laboratory, Golden, CO, USA.
- Josset, C., Babarit, A., & Clement, A. H. (2007). A wave-to-wire model of the searev wave energy converter. In *Proceedings of the institution of mechanical engineers, Part M: Journal of Engineering for the Maritime Environment*: 221 (pp. 81–93).
- Khan, B., Valencia-Palomo, G., Rossiter, J. A., Jones, C., Gondhalekar, R. Long horizon input parameterisations to enlarge the region of attraction of MPC, Optimal Control, Applications and Methods. (Online version available). DOI: 10.1002/oca.2158.
- Knudsen, T., Bak, T., & Soltani, M. (2011). Prediction models for wind speed at turbine locations in a wind farm. *Wind Energy*, 14(7), 877–894. doi:10.1002/we.491.
- Koca, K., Kortenhaus, A., Oumeraci, H., Zanuttigh, B., Angelelli, E., Cantu, M., et al. (2013). Recent advances in the development of wave energy converters. In *Proceedings of the 9th European wave and tidal energy conference (EWTEC)*.
- Kramer, M., Marquis, L., & Frigaard, P. (2011). Performance evaluation of the waves-tar prototype. In *Proceedings of the 10th European wave and tidal energy conference (EWTEC), Southampton*.
- Kuo, B. C. (1995). *Automatic Control Systems* (seventh edition, p. 07632). Englewood Cliffs, New Jersey: Prentice Hall.
- Laino, D. J., & Hansen, A. C. (2002). User's guide to the wind turbine aerodynamics computer software aerodyn. *Tech. rep. TCX-9-29209-01*. Windward Engineering, LC, Salt Lake City, UT, USA. Prepared for the National Renewable Energy Laboratory – NREL, LC.
- Leijon, M. Bernhoff, H. (2006). Wave-power electric device and method. US Patent 7,045,912.
- Leithead, W., & Connor, B. (2000). Control of variable speed wind turbines: design task. *International Journal of Control*, 73(13), 1189–1212. doi:10.1080/002071700417849.
- Levy, E. (1959). Complex curve fitting. *IRE Transaction on Automatic Control*, AC-4, 37–43.
- Li, G., & Belmont, M. R. (2014). Model predictive control of sea wave energy converters—part i: a convex approach for the case of a single device. *Renewable Energy*, 69, 453–463.
- Mahmoud, M., Jiang, J., & Zhang, Y. (2003). Active fault tolerant control systems: stochastic analysis and synthesis. *Lecture Notes in Control and Information Systems*. Berlin, Germany: Springer-Verlag. ISBN: 3540003185.
- Manwell, J. F., McGowan, J. G., & Rogers, A. L. (2002). *Wind energy explained: theory, design, and application*. England: Wiley, West Sussex.
- Matha, D. (2009). Model development and loads analysis of an offshore wind turbine on a tension leg platform, with a comparison to other floating turbine concepts. *Tech. rep. NREL/TP-500-45891*. National Renewable Energy Laboratory, Golden.
- McCabe, A. P., Bradshaw, A., & Widden, M. B. (2005). A time-domain model of a floating body using transforms. In *Proceedings of the 6th European wave and tidal energy conference*.
- McCormick, M. (1981). *Ocean wave energy conversion*. Wiley.
- Merigaud, A., Gilloteaux, J.-C., & Ringwood, J. (2012). A nonlinear extension for linear boundary element methods in wave energy device modelling. In *Proceedings of the ASME 2012 31st international conference on ocean, offshore and arctic engineering (OMAE), Rio de Janeiro, Brazil: Vol. 4* (pp. 615–621). doi:10.1115/OMAE2012-83581.
- Muljadi, E., & Butterfield, C. (1999). Pitch-controlled variable-speed wind turbine generation. In *Proceedings of the 1999 IEEE industry applications society annual meeting, Phoenix, Arizona, USA*. (pp. 470–474).
- Munteanu, I., & Bratcu, A. I. (2008). *Optimal control of wind energy systems: towards a global approach*. Springer. ISBN: 978-1848000797.
- Namik, H., & Stol, K. (2010). Individual blade pitch control of floating offshore wind turbines. *Wind Energy*, 13(1), 74–85. doi:10.1002/we.332.
- Nolan, G., & Ringwood, J. (2005). Assessment of a combined renewable energy resource for Ireland. In *Proc. 6th European wave and tidal energy conference Glasgow*. (pp. 125–247).
- Nolan, G., Ringwood, J., & Holmes, B. (2007). Short term wave energy variability off the west coast of Ireland. In *Proceedings of the 7th European wave and tidal energy conference*. Porto.
- Ochi, M. K. (1998). *Ocean waves: the stochastic approach*. Cambridge University Press.
- Odgaard, P. F. (2012). FDI/FTC wind turbine benchmark modelling. In R. J. Patton (Ed.), *Workshop on Sustainable Control of Offshore Wind Turbines: 1. UK: Centre for Adaptive Science & Sustainability, University of Hull, Hull*.
- Odgaard, P. F., & Johnson, K. (2013). Wind turbine fault diagnosis and fault tolerant control – an enhanced benchmark challenge. *Proceedings of the 2013 American Control Conference – ACC* (pp. 0743–1619). Washington DC, USA: IEEE Control Systems Society & American Automatic Control Council. ISBN: 978-1-4799-0177-7.
- Odgaard, P. F., Shafiei, S. E. Evaluation of wind farm controller based fault detection and isolation, Elsevier Ltd. Books Division, IFAC Workshop Series ISSN: 1474-6670.
- Odgaard, P. F., Stoustrup, J. A benchmark evaluation of fault tolerant wind turbine control concepts. *Transactions on Control Systems Technology* 23 (3)1221–1228.
- Odgaard, P. F., & Stoustrup, J. (2011). Orthogonal bases used for feed forward control of wind turbines. In *Proceedings of the 18th IFAC world congress, IFAC, IFAC, Milan, Italy* (pp. 532–537).
- Odgaard, P. F., & Stoustrup, J. (2013). Fault tolerant wind farm control – a benchmark model. In *Proceedings of the IEEE multi conference on systems and control – MSC2013, Hyderabad, India*. (pp. 1–6).
- Odgaard, P. F., Stoustrup, J., & Kinnart, M. (2013). Fault-tolerant control of wind turbines: A benchmark model. *IEEE Transactions on Control Systems Technology*, 21(4), 1063–6536. doi:10.1109/TCST.2013.2259235. 1168–1182. ISSN.
- Odgaard, P. F., & Stoustrup, J. (2012). Results of a Wind Turbine FDI Competition. In C. Verde, C. M. Astorga, & A. Molina (Eds.), *Proceedings of the 8th IFAC Symposium on Fault Detection, Supervision and Safety of Technical Processes – SAFEPROCESS 2012: Vol. 8* (pp. 102–107). Mexico City, Mexico: National Autonomous University of Mexico. doi:10.3182/20120829-3-MX-2028.00015.
- Ostergaard, K. Z., Stoustrup, J., & Brath, P. (2009). Linear parameter varying control of wind turbines covering both partial load and full load conditions. *International Journal of Robust and Nonlinear Control*, 19(1), 92–116. doi:10.1002/rnc.1340.
- Pao, L. Y., & Johnson, K. E. (2009). A tutorial on the dynamics and control of wind turbines and wind farms. In *Proceedings of the American control conference, 2009 – ACC'09, IEEE, St. Louis, MO, USA* (pp. 2076–2089). doi:10.1109/ACC.2009.5160195. ISSN: 0743-1619. ISBN: 978-1-4244-4523-3
- Pao, L. Y., & Johnson, K. E. (2011). Control of wind turbines. *IEEE Control Systems Magazine*, 31(2), 44–62.
- Pedersen, M. D., & Fossen, T. I. (2012). Efficient nonlinear wind-turbine modeling for control applications: 7. *Proceedings of the 7th Vienna International Conference on Mathematical Modelling (MATHMOD 2012)* (pp. 264–269). Vienna, Austria: IFAC. doi:10.3182/20120215-3-AT-3016.00046.
- Perez, T., & Fossen, T. (2007). Time-domain models of marine surface vessels for simulation and control design based on seakeeping computations. In *Proceedings of the 7th ifac conference on manoeuvring and control of marine craft (CMCM)*.
- Pierson, W., & Moskowitz, L. (1964). A proposed spectral form for fully developed wind seas based on the similarity theory of S.A. Kitaigorodskii. *J. Geophys. Res.*, 69, 5181–5190.
- Pintea, A., Popescu, D. Borne, P. (2010). Proceedings of the 12th IFAC Symposium on Large Scale Systems: Theory and Applications, Vol. 9, IFAC, IFAC, Lille, France, 251–256. 10.3182/20100712-3-FR-2020.00042.
- Plumley, C. E., Leithead, B., Jamieson, P., Bossanyi, E., & Graham, M. (2014). Comparison of individual pitch and smart rotor control strategies for load reduction. In *Journal of physics: conference series: Vol. 524* (p. 012054). doi:10.1088/1742-6596/524/1/012054.
- Prony, R. (1795). Essai experimental et analytique: Sur les lois de la dilatibilité des fluides elastiques et sur celles de la force expansive de la vapeur d'eau et de la vapeur de l'alcool, a differentes temperatures. *Paris J. l'Ecola Polytechnique*, 1, 24–76.
- Quine, B., Uhlmann, J., & Durrant-Whyte, H. (1995). Implicit jacobians for linearised state estimation in nonlinear systems. In *Proceedings of the American control conference* (pp. 1645–1646).

- 2058 Rasmussen, F., Hansen, M., Thomsen, K., Larsen, T., Bertagnolio, F., Johansen, J., ...
 2059 Hansen, A. (2003). Present status of aeroelasticity of wind turbines. *Wind Energy*,
 2060 6(3), 213–228. doi:10.1002/we.98.
- 2061 Richter, M., Magaña, M., Sawodny, O., & Brekken, T. (2013a). Nonlinear model predictive
 2062 control of a point absorber wave energy converter. *Sustainable Energy, IEEE Trans-*
 2063 *actions*, 4(1), 118–126.
- 2064 Richter, M., na, M. E. M., Sawodny, O., & Brekken, T. K. (2013b). Nonlinear model
 2065 predictive control of a point absorber wave energy converter. *Sustainable Energy, IEEE*
 2066 *Transactions*, 4(1), 118–126.
- 2067 Ringwood, J., Bacelli, G., & Fusco, F. (2014). Energy-maximizing control of wave-energy
 2068 converters: the development of control system technology to optimize their oper-
 2069 ation. *Control Systems, IEEE*, 34(5), 30–55.
- 2070 Schlipf, D., Sandner, F., Raach, S., Hocke, V., Matha, D., & Cheng, P. W. (2013). Nonlin-
 2071 ear model predictive control of floating wind turbines. In *Proceedings of the 23rd*
 2072 *international offshore and polar engineering – ISOPE 2013, ISOPE, Anchorage, USA.*
 2073 (pp. 440–446).
- 2074 Shek, J., Macpherson, D., & Mueller, M. (2008). Phase and amplitude control of a linear
 2075 generator for wave energy conversion. In *Proceedings of the 4th IET conference on*
 2076 *power electronics, machines and drives (PEMD)* (pp. 66–70).
- 2077 Shek, J. K.-H., Macpherson, D. E., Mueller, M. A., & Xiang, J. (2007). Reaction force con-
 2078 trol of a linear electrical generator for direct drive wave energy conversion. *IET*
 2079 *renewable power generation*, 1(1), 17–24.
- 2080 Shi, F., & Patton, R. J. (2015). An active fault tolerant control approach to an offshore
 2081 wind turbine model. *Renewable Energy*, 75(1), 788–798. doi:10.1016/j.renene.2014.
 2082 10.061.
- 2083 Simani, S., Fantuzzi, C., & Patton, R. J. (2003). Model-based fault diagnosis in dynamic
 2084 systems using identification techniques. *Advances in Industrial Control*: 1 (1st). Lon-
 2085 don, UK: Springer–Verlag. ISBN: 1852336854.
- 2086 Simani, S., & Castaldi, P. (2014). Active actuator fault tolerant control of a wind turbine
 2087 benchmark model. *International Journal of Robust and Nonlinear Control*, 24(8–9),
 2088 1283–1303. John Wiley. doi:10.1002/rnc.2993.
- 2089 Simani, S., Farsoni, S., & Castaldi, P. (2015a). Fault-Tolerant control of offshore wind
 2090 farm installations via adaptive nonlinear filters. *Proceedings of the International*
 2091 *Conference on Systems Engineering – ICSE 2015, Control Theory and Applications Cen-*
 2092 *tre, Faculty of Engineering and Computing, Coventry, UK: Coventry University Tech-*
 2093 *nology Park, IEEE.* (Accepted).
- 2094 Simani, S., Farsoni, S., Castaldi, P., & Mimmo, N. (2015b). Active fault-tolerant control of
 2095 offshore wind farm installations. In *Proceedings of the 9th IFAC symposium on fault*
 2096 *detection, supervision and safety for technical processes – SAFEPROCESS'15, IFAC, paris,*
 2097 *france.* Invited paper. (Accepted).
- 2098 Soerensen, H. (2003). Development of wave dragon from scale 1:50 to prototype. In
 2099 *Proceedings of the 5th European wave energy conference* (pp. 110–116). HMRC, Cork.
- 2100 Soulard, T., Babarit, A., Borgarino, B., Wynn, M., & Harismendy, M. (2013). C-hyp: a
 2101 combined wave and wind energy platform with balanced contributions. In *Proceedings*
 2102 *of the ASME 32nd international conference on ocean, offshore and arctic engineering*
 2103 *(OMAE2013), Nantes, France.*
- 2104 Taghipour, R., Perez, T., & Moan, T. (2008). Hybrid frequency time domain models for
 2105 dynamic response analysis of marine structures. *Ocean Engineering*, 35, 685–705.
- 2106 Taylor, C. J., Stables, M. A., Cross, P., Gunn, K., & Aggidis, G. A. (2009). Linear and nonlin-
 2107 ear modeling and control of a power take-off simulation for wave energy conver-
 2108 sion. In *Proceedings of the 8th European wave and tidal energy conference, EWTEC.*
- 2109 Teillant, B., Costello, R., Weber, J., & Ringwood, J. (2012). Productivity and economic
 2110 assessment of wave energy projects through operational simulations. *Renewable*
 2111 *Energy*, 48, 220–230.
- 2112 Trapanese, M. (2008). Optimization of a sea wave energy harvesting electromagnetic
 2113 device. *Magnetics, IEEE Transactions*, 44(11), 4365–4368.
- 2114 Valencia-Palomo, G., Rossiter, J. A., & Lopez-Estrada, F. (2014). Improving the feed-
 2115 forward compensator in predictive control for setpoint tracking. *ISA Transactions*,
 2116 53(3), 755–766. doi:10.1016/j.isatra.2014.02.009.
- 2117 WAMIT (2002). WAMIT user manual.
- 2118 Whittaker, T., & Folley, M. (2012). *Near-shore oscillating wave surge converters and the*
 2119 *development of oyster* (pp. 345–364). Phil. Trans. R. Soc. A.
- 2120 Yemm, R., Pizer, D., Retzler, C.. Floating apparatus and method for extracting power from
 2121 sea waves. note US Patent No. 6476511.
- 2122 Zhang, Y., & Jiang, J. (2008). Bibliographical review on reconfigurable fault-tolerant
 2123 control systems. *Annual Reviews in Control*, 32, 229–252.
- 2124 Zurkinden, A., Guerinel, M., Alves, M., & Damkilde, L. (2013). Theoretical investigation
 2125 of a wave energy system by applying reactive control using stochastic analysis of
 2126 the wave state. In *Proceedings 11th European wave and tidal energy conference, Aal-*
 2127 *borg, Denmark.*
- John V. Ringwood** received the Hons. Diploma in Electrical Engineering from Dublin
 2128 Institute of Technology, Dublin, Ireland, the BSc(Eng) from Trinity College, Dublin, and
 2129 the Ph.D. degree in control systems from Strathclyde University, Glasgow, U.K. Previ-
 2130 ously, he was with the School of Electronic Engineering, Dublin City University, Dublin,
 2131 Ireland, and has held visiting positions with Massey University, New Zealand, and
 2132 Auckland University, Auckland, New Zealand. He is currently Professor in the Depart-
 2133 ment of Electronic Engineering and Director of the Centre for Ocean Energy Research,
 2134 Maynooth University, Ireland. John is a Chartered Engineer and a Fellow of Engineers
 2135 Ireland.
- Silvio Simani** received the M.Sc. degree in Electronic Engineering from the University
 2137 of Ferrara, Ferrara, Italy, in 1996, and the Ph.D. degree in Information Sciences (Auto-
 2138 matic Control area) from the University of Modena and Reggio Emilia, Modena, Italy,
 2139 in 2000. Since 2000, he has been a member of the IFAC SAFEPROCESS Technical Com-
 2140 mittee. In 2002, he became an Assistant Professor with the Department of Engineering,
 2141 University of Ferrara, where he has been an Associate Professor since 2014. His research
 2142 interests include fault diagnosis, fault-tolerant control, and system identification, on
 2143 which he has published about 160 refereed journal and conference papers, as well as
 2144 two books and several chapters.